OAK RIDGE NATIONAL LABORATORY LIBRARIES
3 4456 0549369 5

CENTRAL RESEARCH LIBRARY
DOCUMENT COLLECTION

OAK RIDGE NATIONAL LABORATORY

operated by

UNION CARBIDE CORPORATION

for the

U.S. ATOMIC ENERGY COMMISSION

ORNL-TM-642

131

UNIT OPERATIONS SECTION

MONTHLY PROGRESS REPORT

JULY 1963

CENTRAL RESEARCH LIBRARY
DOCUMENT COLLECTION
LIBRARY LOAN COPY
DO NOT TRANSFER TO ANOTHER PERSON
If you wish someone else to see this document, send in name with document and the library will arrange a loan.

NOTICE

This document contains information of a preliminary nature and was prepared primarily for internal use at the Oak Ridge National Laboratory. It is subject to revision or correction and therefore does not represent a final report. The information is not to be abstracted, reprinted or otherwise given public dissemination without the approval of the ORNL patent branch, Legal and Information Control Department.

LEGAL NOTICE

This report was prepared as an account of Government sponsored work. Neither the United States, nor the Commission, nor any person acting on behalf of the Commission:

A. Makes any warranty or representation, expressed or implied, with respect to the accuracy, completeness, or usefulness of the information contained in this report, or that the use of any information, apparatus, method, or process disclosed in this report may not infringe privately owned rights; or

B. Assumes any liabilities with respect to the use of, or for damages resulting from the use of any information, apparatus, method, or process disclosed in this report.

As used in the above, "person acting on behalf of the Commission" includes any employee or contractor of the Commission, or employee of such contractor, to the extent that such employee or contractor of the Commission, or employee of such contractor prepares, disseminates, or provides access to, any information pursuant to his employment or contract with the Commission, or his employment with such contractor.

ORNL-TM-642

UNIT OPERATIONS SECTION MONTHLY PROGRESS REPORT

July 1963

CHEMICAL TECHNOLOGY DIVISION

M. E. Whatley

P. A. Haas
R. W. Horton
A. D. Ryon
J. C. Suddath
C. D. Watson

Date Issued

NOV 8 1963

OAK RIDGE NATIONAL LABORATORY
Oak Ridge, Tennessee
Operated by
UNION CARBIDE CORPORATION
for the
U. S. Atomic Energy Commission

OAK RIDGE NATIONAL LABORATORY LIBRARIES
3 4456 0549369 5

ABSTRACT

Foam has been effectively condensed by passing it through an orifice at a velocity sufficient to cause at least 50% reduction of pressure. Orifice diameters of 0.015, 0.100, and 0.250 cm were equally efficient for foam composed of 0.05 to 0.08 cm diameter bubbles. Small spherical thoria beads having high resistance to crushing and low internal porosity were prepared by dispersing a 4.5 M thoria sol through an orifice into a mixture of carbon tetrachloride and isopropyl alcohol producing gel beads which were calcined at 1000°C. The rate-controlling mechanisms for the sorption of uranium hexafluoride on sodium fluoride pellets are: transfer across the gas film, diffusion in the pore space and diffusion through the UF_6-NaF complex. Experimental data were correlated on the basis of a model involving simultaneous diffusion and irreversible reaction. Two high level waste calcinations runs using simulated FTW-65 Purex waste containing four times the normal sodium content are reported.

CONTENTS

		Page
	Abstract	2
	Previous Reports in this Series for the Year 1963	4
	Summary	5
1.0	Foam Separation Studies - Waste Processing Development	7
2.0	Thorium Utilization Studies	11
3.0	Volatility Studies	18
4.0	Waste Processing Studies	29

Previous Reports in this Series for the Year 1963

January	ORNL-TM-541
February	ORNL-TM-581
March	ORNL-TM-586
April	ORNL-TM-608
May	ORNL-TM-613
June	ORNL-TM-628

All previous reports in this series are listed in the June 1963 report, ORNL-TM-628, from the beginning, December 1954.

SUMMARY

1.0 FOAM SEPARATION STUDIES - WASTE PROCESSING DEVELOPMENT

Experimental results show that foams are easily condensed while passing through an orifice with upstream/downstream pressure ratios of two or greater. The 0.015, 0.100, and 0.250 cm diam orifices all gave residual foam volumes of about 0.001 times the inlet foam volumes for foams of 0.05 to 0.08 cm mean diameters. As compared to impingement on a Teflon sheet 2 to 3 inches from the orifice, the amount of uncondensed foam was slightly decreased by placing the sheet 24 in. from the orifice and was slightly increased by use of a glass wall in place of the Teflon sheet. The 24 in. diam foam column (the proposed LLW pilot plant column diameter) was operated at flows up to 80 liters/min of foam and 13 liters/min of liquid. The amount of channeling appeared acceptable at 5 liters/min or less liquid and 50 liters/min or higher gas flow rates; an improved liquid feed distributor will be necessary for higher liquid flow rates.

2.0 THORIUM UTILIZATION STUDIES

Spherical beads of thorium oxide gel in the size range 100 to 1000 μ were prepared by passing a 4.5 M thoria sol through a 0.006-in.-diam orifice into a CCl_4-15 to 17 vol % isopropyl alcohol solution, which fluidized and dried the resultant droplets. The gel beads were further dried and calcined at 1000°C to give thoria spheres having high resistance to crushing and little internal porosity. Surface active impurities which were accidentally present appear necessary to prevent coalescence and to maintain the spherical drop shape throughout drying.

3.0 VOLATILITY STUDIES

The removal of uranium hexafluoride from a gas stream containing uranium hexafluoride and nitrogen by pelleted sodium fluoride was investigated by the use of differential-beds of pellets. Experimental data on the rate and extent of sorption was obtained in the temperature range 29 to 100°C and uranium hexafluoride concentration range 0.57 to 10.9 mole per cent uranium hexafluoride.

The results of this study indicate that the rate-controlling mechanisms are transfer of uranium hexafluoride across a stagnant gas film surrounding the pellet, diffusion of gaseous uranium hexafluoride in the pore space of the pellet, and diffusion of uranium hexafluoride through a layer of uranium hexafluoride-sodium fluoride complex covering unreacted sodium fluoride in the interior of the pellet. The crystalline density of the complex $UF_6 \cdot 2NaF$ was determined to be 4.13 g/cc which indicates that incomplete reaction of the sodium fluoride will occur for pellets in which the initial volume void fraction is less than 0.807.

A model was devised to represent the sorption of uranium hexafluoride by a single pellet of sodium fluoride and differential equations based on the model were written. A general method of solution of the partial

differential equation describing simultaneous diffusion and irreversible reaction with variable diffusivity and reaction rate constant was derived for systems in which a steady-state type solution is valid. The experimental data were correlated on the basis of the model with a root-mean square error of 9.5% for all points. The resulting computer code and associated data may be used for design of sorber systems such as fixed or moving beds.

The effective capacity of 1/8-in. right circular cylindrical pellets of NaF for UF_6 was found to decrease with increasing temperature; at 29°C a capacity of 1.13 g UF_6/g NaF was observed whereas the capacity at 100°C was only 0.64 g UF_6/g NaF. A model-predicted result of a 35% decrease in capacity for pellets having an initial void fraction of 0.45 was observed experimentally as the surface area was increased from 0.86 to 1.1 m^2/g.

4.0 WASTE PROCESSING STUDIES

Two tests, R-77 and R-78, have been completed using FTW-65 Purex waste with four times the normal amount of sodium (1.2 M sodium). The sodium was added as sodium sulfate so that there would be a 0.6 M sodium sulfate concentration. The operation of this type of feed was fairly difficult because the feed tended to foam and therefore more entrainment in the off-gas line was encountered than with regular FTW-65 Purex.

The average feed rates for the two tests were 18.6 and 19.2 liters/hr, respectively. The resulting solid had a bulk density for the two tests of 1.26 and 1.39 g/cc, respectively. The reason R-78 had a higher density was that 904 liters of feed was used for that test whereas only 726 liters of feed was used for test R-77. The calcium added to complex the sulfate for both tests was 10% of the total sulfate. The sulfate found in the calciner condensate of test R-77 was 0.07% of the total sulfate fed to the system. The sulfate in the calciner condensate in R-78 was much higher, about 25%, due to the large amount of carryover. This type of feed can be handled satisfactorily with the regular calciner operating procedure, however, a larger de-entraining section in the calciner pot would be advisable.

1.0 FOAM SEPARATION STUDIES - WASTE PROCESSING DEVELOPMENT

P. A. Haas

1.1 Foam Separation - P. A. Haas, D. A. McWhirter

Engineering studies for design and application of foam separation columns were continued with the emphasis on the scale up of components for the 24 in. diam column proposed for a Low Level Waste pilot plant. The 6 and 24 in. diam columns were operated with orifices as simple and easily scaled-up foam breakers.

Orifice Foam Breakers. The idea of an orifice as a foam breaker was developed from consideration of the foam breaking mechanism in the sonic, cyclone, and centrifugal foam breakers. The sonic foam breaking mechanism is ascribed to pressure cycling effects.[1] The 2 to 1 inlet to outlet pressure ratio found necessary to make a cyclone an effective foam breaker would produce a very rapid pressure change. Foam flowing through either a stationary fine mesh screen or a coarse screen centrifuge bowl are broken very poorly as compared to a fine screen centrifuge bowl. This could be attributed to a pressure change as the foam leaves the centrifugal field in the bowl. Since sharp pressure changes and even pressure discontinuities are possible in an orifice, the performance of orifices as foam breakers was tested.

Experimental data were collected for four orifice diameters using foam from extra coarse porosity fritted glass disc gas spargers. Foam generated from 200 to 275 ppm Trepolate F-95 solution was drawn through the orifice by vacuum with the top of the column vented to the atmosphere (Fig. 1.1). The amount of uncondensed foam was measured by operating the orifice for 2 to 5 minutes and then venting the vacuum pot and discharging the liquid and foam into a graduate. The orifice diameter, the foam rate, the pressure drop across the orifice, the foam density, the distance from the orifice to the vacuum chamber wall, and the wall material were varied.

The experimental results show that foams are easily condensed by an orifice with residual foam volumes of about 0.001 the inlet volumes for the well drained foams (Table 1.1). Pressure drops from atmospheric for the inlet foam to one-half atmosphere in the vacuum pot were adequate. The same pressure ratio would probably apply at other pressures; i.e., an upstream to downstream pressure ratio of two is probably adequate. With the inlet foam at atmospheric pressure, condensation was less complete for 30 or 25 cm of Hg pressure drop than for 50 or 65 cm Hg, and become very poor for lower pressure drops.

The results indicate that the condensation occurs as the bubbles pass through the orifice and that orifices smaller than the bubble and impingement of the bubbles on a surface are not necessary. The condensation of

[1] R. M. G. Boucher and A. L. Weiner, "Sonic Defoaming-Its Present Status," Food Processing, October 1962.

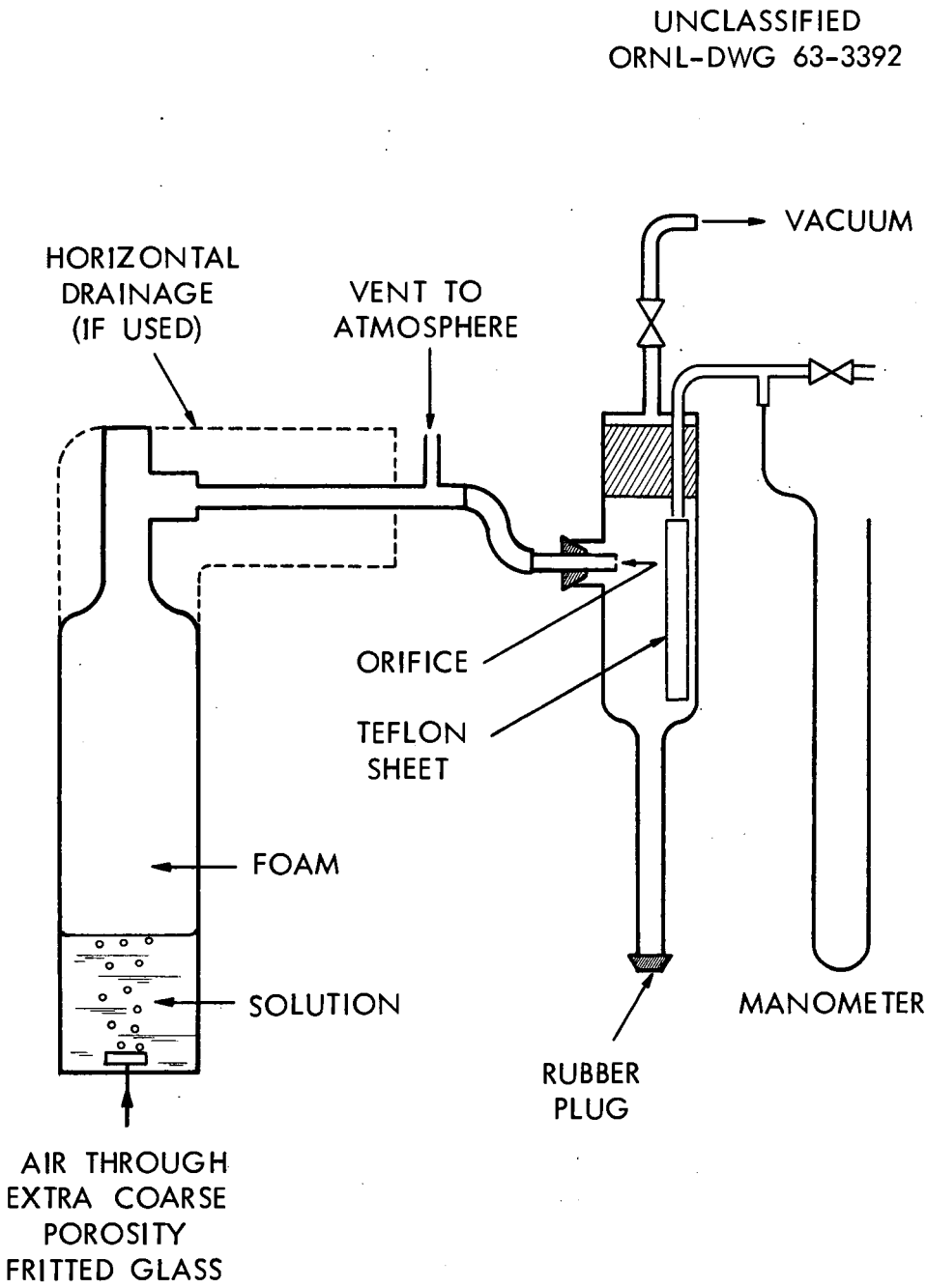

Fig. 1.1 Orifice Foam Breaker Test Apparatus.

Table 1.1. Orifice Foam Breaker Test Conditions and Results.

Solution: 275 ppm Trepolate F-95 and 0.002 N NaOH.

Orifice Opposing Wall				Foam Column		Pressure Drop	Foam Rate	Foam Density	Average Bubble Diam	Fraction of Uncondensed Foam
No.	Diam (cm)	Material	Distance	Diam (in.)	Foam Drainage Flow	(cm Hg)	(cc/min)	(mg/cc)	(cm)	(cc/cc)
Twelve	0.015	Glass	~3	6	Horizontal	~65	1000	~3	0.05	< 0.001
One	0.100	Glass	~2	6	Horizontal	~65	5600	4	0.07	0.0016
							3700	3	0.06	0.0005
						50	5600	4	0.07	0.0019
							3700	3	0.06	0.0011
						30	5600	4	0.07	0.0012
							3700	3	0.06	0.0010
						25	3700	3	0.06	0.0040
		Teflon	~2	6	Horizontal	~65	5600	4	0.07	0.0005
							3700	3	0.06	0.0006
						30	5600	4	0.07	0.0012
							3700	3	0.06	0.0014
		Teflon	~2	6	Vertical	~65	3700	12	0.07	0.0040
							1900	9	0.06	0.0016
							700	4	0.05	< 0.0005
						50	3700	12	0.07	0.0040
						30	3700	12	0.07	0.0032
							1900	9	0.06	0.0021
							700	4	0.05	< 0.0005
		Teflon	~24	6	Vertical	~65	3700	12	0.07	0.0016
							1900	9	0.06	0.0013
						30	3700	12	0.07	0.0027
							1900	9	0.06	0.0048
One	0.250	Teflon	~3	24	Vertical	~60	40000	4	0.07	0.0010
							32000	3.5	0.06	0.0011
							16000	1	0.05	0.0005
							8000	0.5	0.05	0.0005
One	0.32	Teflon		24	Vertical	~50	48000	6	0.07	-

foam was about equally efficient for 0.015, 0.100, and 0.250 cm diam orifices. The 0.015 cm diam would be smaller than nearly all the bubbles while the 0.250 cm diam would be larger than nearly all the bubbles (mean bubble diameters of 0.05 to 0.08 cm). For most of the tests, the stream from the orifices impinged on a Teflon sheet placed 2 to 3 inches from the orifice. The amount of uncondensed foam was slightly decreased by placing the orifice 24 in. from the Teflon sheet. The amount of uncondensed foam was slightly greater for a glass surface than for the Teflon sheet. It appeared that the foam bubbles broke before they hit the surface and that the liquid striking the surface caused some formation of new foam bubbles depending on the material and position of the surface.

The drier foams from lower foam rates or better drainage gave smaller fractions of uncondensed foam. This may have been due to less formation of new foam bubbles on the Teflon surfaces.

24 in. Diam Column. The 24 in. diam foam column (see April Unit Operations Monthly Report) with a feed distributor of nineteen tubes on a 5 in. triangular spacing was operated at higher gas rates using the 0.25 and 0.31 cm diam orifice foam breakers. The amount of channeling decreased as the gas (i.e. foam) rate was increased. With the present feed distributor and 50 liters/min of foam, the flow was good with little channeling at 5 liters/min of liquid (25 gal/sq ft hr), but channeling was very bad at 13 liters/min (66 gal/sq ft hr). Channeling was less, but still excessive, at 13 liters/min for 80 liters/min foam. A feed distributor using a larger number of tubes on a closer spacing should be designed and mocked-up for the 24 in. diam LLW pilot plant column.

2.0 THORIUM UTILIZATION STUDIES

P. A. Haas

Procedures and equipment are being developed to adapt the Sol-Gel process to give a variety of product compounds and characteristics. The conversion of thorium nitrate to a thoria sol by this process is a very cheap, simple, and dependable operation. Rounded thoria or thoria-urania beads of 100 to 1000 μ diam without any sharp corners or crevices would be excellent for coating with pyrolytic carbon coatings or for other dispersion fuels. Since dried sol-carbon black mixtures react at relatively low temperatures because of the large surface area of each component, spherical thoria-urania gel-carbon black beads would give spherical thorium carbide-uranium carbide beads at temperatures of 1000°C lower than those used in other processes. Therefore, procedures are being developed for conversion of sols to dried gel beads of 100 to 1000 μ diam.

2.1 Thoria Micro-Spheres - S. D. Clinton, L. J. Hirth, D. A. McWhirter

Spherical thorium-oxide gel beads in the size range of 200 to 800 microns were made by fluidizing and drying 4.5 M ThO_2 sol droplets in a CCl_4-isopropyl alcohol solution (17 vol % alcohol). The sol droplets were formed by passing ThO_2 sol through a 6 mil diam orifice. The sol beads were fluidized and dried in a 2 ft length of tapered glass pipe in which the average upward fluid velocity varied from 1.05 to 0.12 ft per sec along the tapered length.

A 6 mil diam orifice attached to a 12 in. length of 1/2 in. SS tubing was used to feed the ThO_2 sol and form the sol droplets. During run A, 18 cc of 4.6 M ThO_2 sol (Density = 2.15 g/cc) was fed through the orifice in approximately 60 minutes with only the aqueous sol height in the tube acting as a driving force across the 6 mil diam hole. The sol droplets were formed in the organic solution with most of the drops in the size range of 800 to 1000 microns.

The CCl_4-17 vol % isopropanol solution was circulated upward through a 2 ft length of tapered glass pipe column which varied from 1 in. ID at the bottom to 3 in. ID at the top. While ThO_2 sol was being fed to the column during run A, the organic flow rate was maintained at a constant value of 2.56 gpm. The average organic velocity varied from 1.05 to 0.12 ft per sec along the tapered length corresponding to Reynold's numbers of 10,000 to 3,300.

The sol droplets were apparently dried to a gel state in about 5 min after formation, however, no gel particles were removed until 18 cc of sol had been introduced into the column and the organic flow rate subsequently reduced to 1.53 gpm. Eleven samples of ThO_2 gel particles were removed from the column at reduced organic flow rates (Table 2.1). These particles appeared to be spherical and exhibited no signs of particle agglomeration. All of the ThO_2 samples were heated overnight at 80°C,

Table 2.1. Size Classification of Thoria Gel Beads by Controlling the Organic Flow Rate

Run A Sample No.	Avg Organic Velocity at 1 in. ID (ft/sec)	Reynold's Number	After Heating at 80°C Observed Size (microns)	Weight (g)
1, 2, 3	0.63	6100	500-1000	3.47
4, 5	0.57	5500	500-900	9.49
6	0.52	5100	600-800	4.54
7	0.45	4400	500-700	2.24
8	0.40	3800	500-600	1.43
9	0.29	2800	300-500	0.95
10	0.17	1700	250-300	0.38
11	0.00	0	150-250	0.09
				22.59

and subsequently three of the samples (A-4, 5, 6) were fired at 1000°C for 16 hrs. The toluene density of the ThO_2 gel beads heated at 80°C was 7.7 g/cc and increased to 9.6 g/cc after firing at 1000°C. On firing to 1000°C the weight of the 80°C heated beads decreased by about 4.0%.

Two photographs of the ThO_2 gel spheres sample No. A-8 (Figs. 2.1 and 2.2) with different exposures indicate the general shape of the particles. In the cross-section view of A-8 (Fig. 2.3), the outer ThO_2 shell (100 to 150 microns thick) was apparently formed while drying in contact with the organic solution. The inner ThO_2 core was probably in a sol state when the particles were removed from the organic solution, however, on heating to 80°C additional water was removed causing the inner core to solidify. From a cross-section view of ThO_2 particles (sample No. A-5) after firing at 1000°C (Fig. 2.4) the ThO_2 appears to be homogeneous and does not exhibit the shell effect of the 80°C heated particles. Several surface cracks are apparent in the cross-section of the high fired-ThO_2 beads, however, these cracks do not seem to be detrimental to the particle crushing strength.

Attempts to duplicate run A with fresh CCl_4-isopropanol solution have failed due to sol droplets coalescing and wetting the glass column wall. In run A the CCl_4 leached the plasticizer from polyvinylchloride tubing connecting the pump, rotameter, and column. Apparently the plasticizer was a surface active agent preventing drop coalescence and glass wetting, however, the interfacial tension between the aqueous sol droplet and the organic solution remained high enough during drying to maintain the spherical shape. The effects of surface active materials on the sol-organic interfacial phenomena are being studied to determine the conditions necessary for duplicating the results of run A.

UNCLASSIFIED
ORNL-PHOTO M-3523

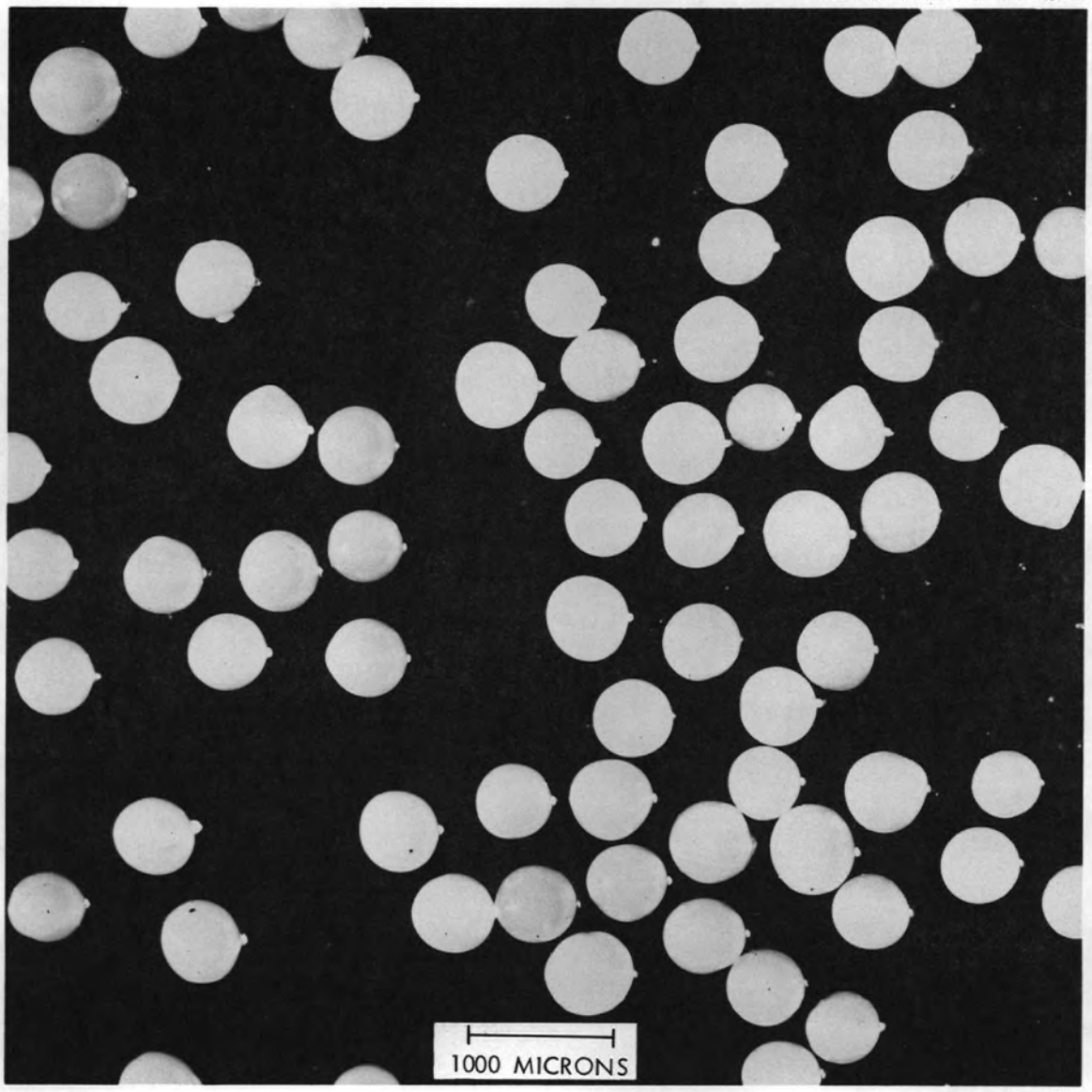

Fig. 2.1 Thoria Gel Spheres Formed by Drying Thoria Sol Droplets in CCl_4-Isopropanol and Heating to 80°C. Sample A-8.

UNCLASSIFIED
ORNL-PHOTO M-3523

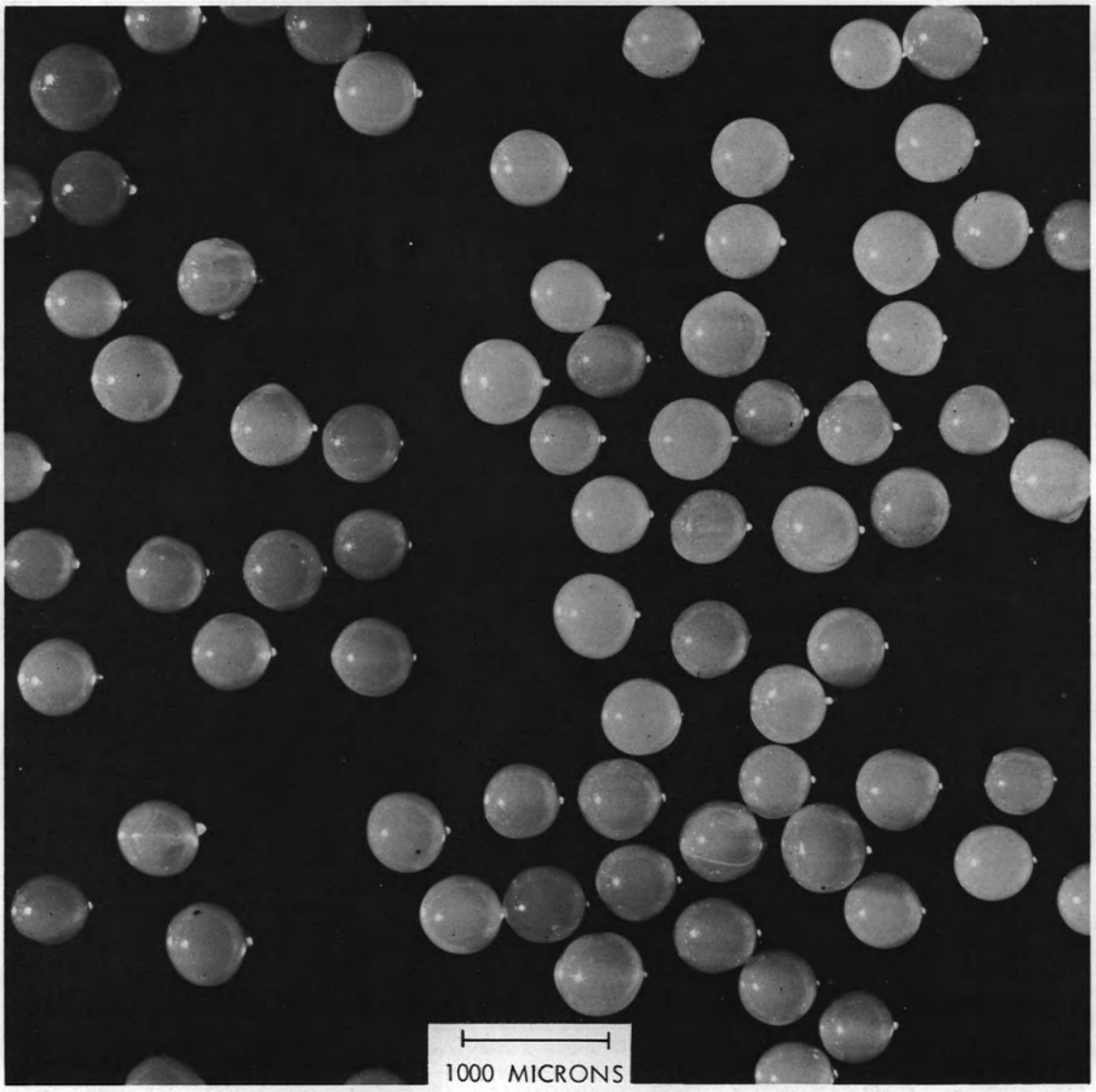

Fig. 2.2 Thoria Gel Spheres Formed by Drying Thoria Sol Droplets in CCl_4-Isopropanol and Heating to 80°C. Sample A-8.

UNCLASSIFIED
ORNL-PHOTO M-3527

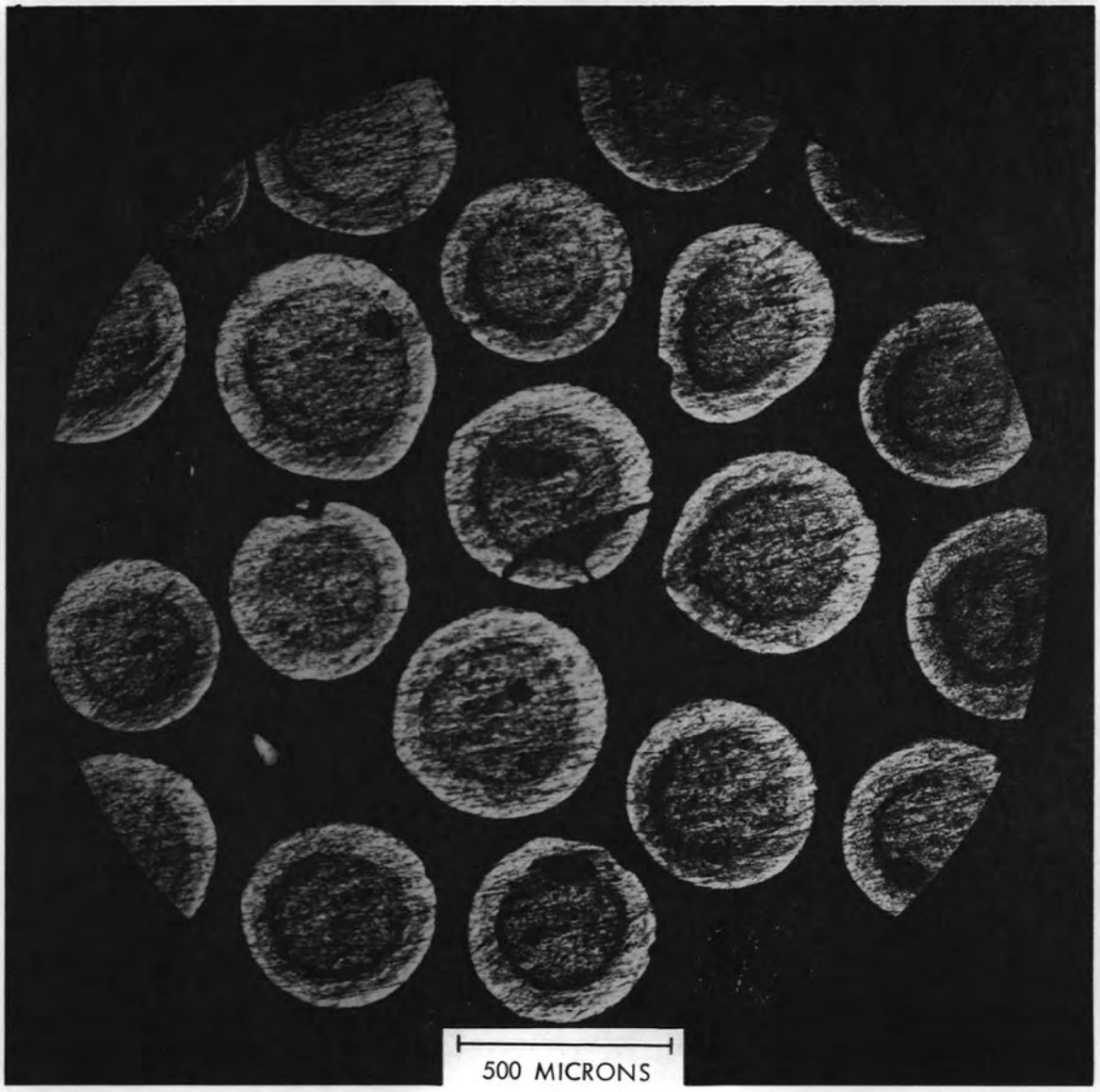

Fig. 2.3 Cross-Section of Thoria Gel Spheres Formed by Drying Thoria Sol Droplets in CCl_4-Isopropanol and Heating to 80°C. Sample A-8.

UNCLASSIFIED
ORNL-PHOTO M-3529

Fig. 2.4 Cross-Section of Thoria Spheres Formed by Drying Thoria Sol Droplets in CCl_4-Isopropanol and Firing to 1000°C. Sample A-5.

3.0 VOLATILITY STUDIES

R. W. Horton

3.1 Sorption of UF_6 on NaF - L. E. McNeese

Determination of the factors which control the rate of removal of UF_6 from a flowing gas stream by a fixed bed of NaF is needed for rational design of fixed bed sorbers which are to operate over wide ranges of conditions. In a previous report (September 1961 Unit Operations Monthly Progress Report), discussion was given of a physical model which explained the observed characteristics of the sorption process. The model was based on two key ideas: first, that the pores in pelleted NaF would be filled with the UF_6-NaF complex prior to complete reaction of the NaF, and secondly, that the diffusivity in a gas varies as $T^{3/2}$ whereas the diffusivity through a crystalline solid varies as $e^{-E/RT}$. A partial differential equation based on the model was derived from which the loading on a single pellet could be calculated.

To provide data for checking the model, a series of runs was made for measuring UF_6 loading on a single layer of NaF pellets (commercial grade from Harshaw Chemical Company) through which a N_2-UF_6 stream was flowing (December 1961 Unit Operations Monthly Progress Report). In a given series, temperature, UF_6 concentration, and gas flow rate were held constant.

The partial differential equation which was derived contains three quantities which are dependent on the amount of UF_6 that has accumulated at a point. These are the point values of the volume void fraction, the effective diffusivity, and the reaction rate constant. A numerical method was devised for solution of the partial differential equation which allowed an arbitrary dependence of the quantities listed above on the UF_6 loading (April 1963 Unit Operations Monthly Progress Report).

The crystalline density of the complex $UF_6 \cdot 2NaF$ was determined to be 4.13 g/cm^3. Based on this measurement, the density of crystalline NaF, and the initial volume void fraction of the NaF pellets (0.45), a relation for the volume void fraction as a function of UF_6 loading was derived which is

$$\epsilon = 0.45(1 - 168.1\ q)$$

where

ϵ = volume void fraction

q = point UF_6 loading, g moles/cm^3 pellet.

The two other relations (effective diffusivity and reaction rate constant) contain five constants whose values were determined by a parameter search. The relation for the point diffusivity is

$$D_e = D_{UF_6-N_2}\ \gamma\epsilon^n$$

and the relation for the point reaction rate constant is

$$\beta = ae^{-E/RT}\ e^{-bq}$$

where

$D_{UF_6-N_2}$ = diffusivity of UF_6 in N_2

γ, n, a, E, b = constants

R = gas constant

T = time.

In order to accomplish the parameter search, the relations discussed above were coded in FORTRAN for a finite-difference solution using the IBM-7090 computer. For most of the computer calculations, the spherical pellet upon which the model is based was divided into forty shells of equal volume; the length of each time increment was chosen such that the maximum change in the point reaction rate constant or the point diffusivity during the time increment would be 5% of its current value or less. In this method of solution, the time increments were short initially (approximately 0.5 sec) and increased continuously as the solution progressed so that after approximately 1 hour of computed time had been accumulated, time increments of approximately 100 sec were observed.

The calculational method was observed to converge to within 1% of the analytical solution for β and D_e of a functional form similar to the experimental case when forty equal-volume shells were used. As a further check on convergence, a number of the calculations were repeated using eighty shells and a maximum change in the current value of β or D_e of 2.5%; a difference of less than 1% in calculated values for uranium hexafluoride loading were observed for the two cases.

The relations which resulted from the parameter search are

$$D_e = 0.369\ D_{UF_6-N_2}\ \epsilon^2$$

$$\beta = 6.25 \times 10^6\ e^{-7000/RT}\ e^{-1390q}\ .$$

A comparison of the experimental data on variation of pellet loading with time with model-predicted values for the loading using these rate relations is shown in Figs. 3.1 through 3.5. Experimental and calculated values for pellet capacity as a function of temperature are shown in Fig. 3.6. The root-mean-square error for all points in the study was 9.5%; the largest error for a single point was 31%.

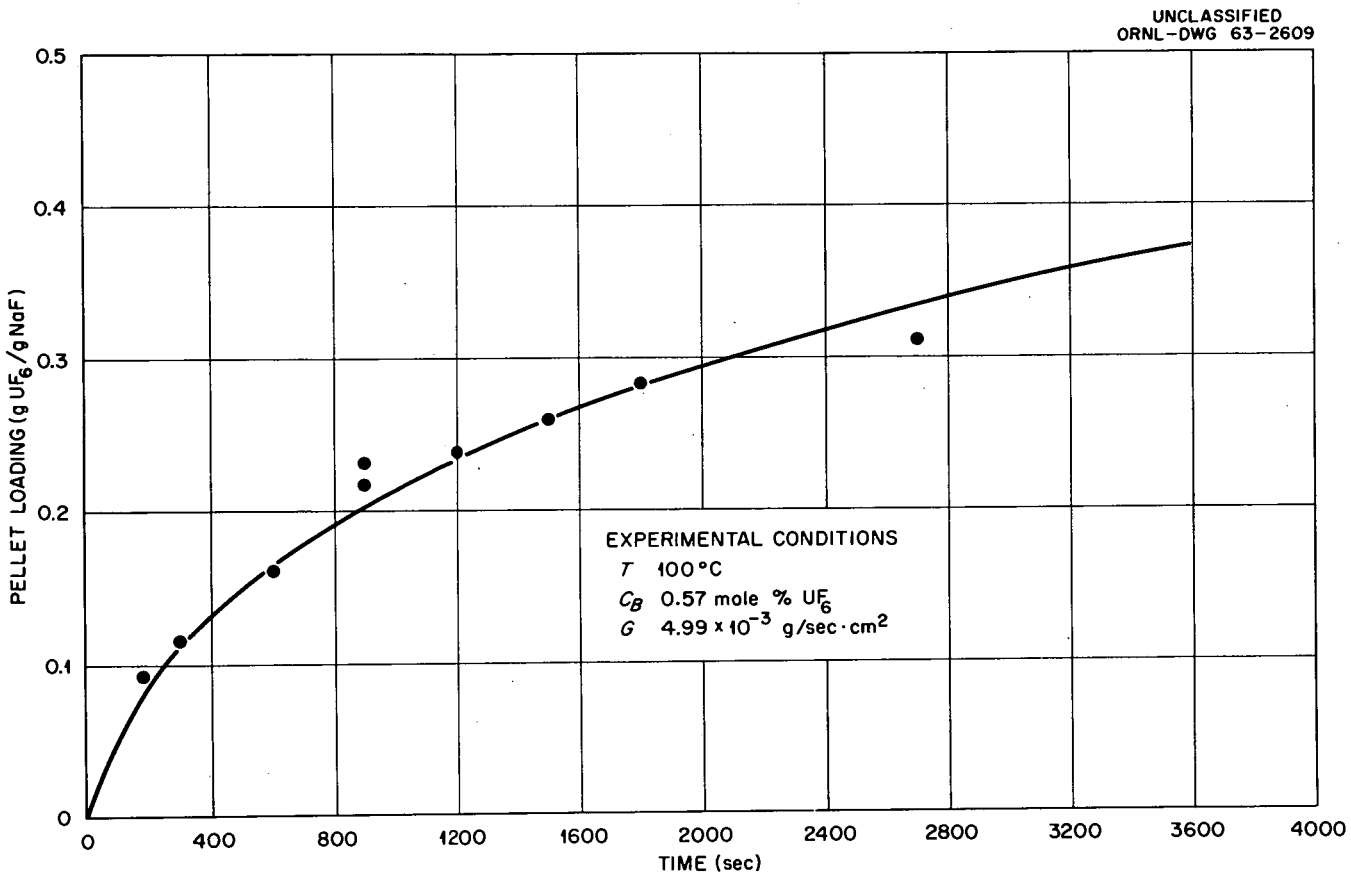

Fig. 3.1 Comparison of Experimental and Model-Predicted Data Showing Variation of Pellet Loading with Time at 100°C and 0.57 Mole Per Cent Uranium Hexafluoride.

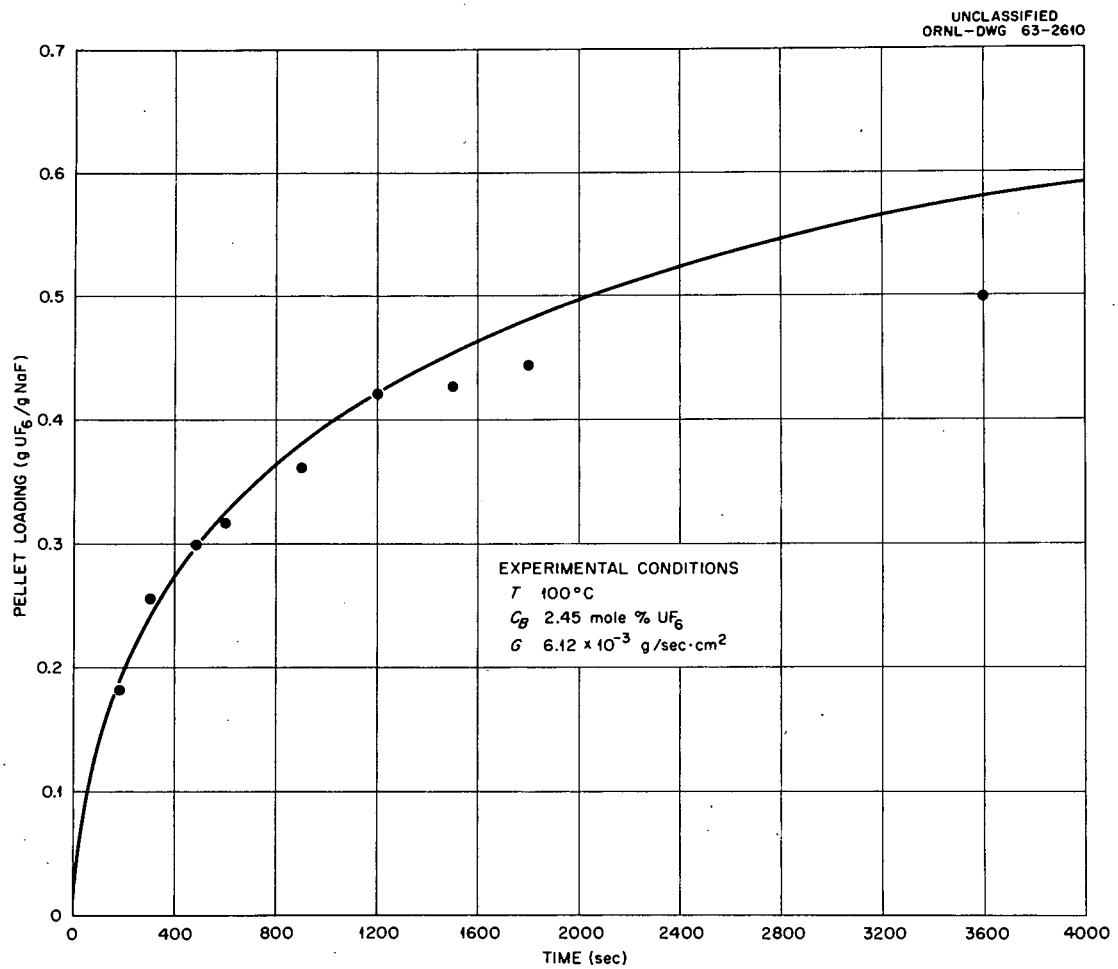

Fig. 3.2 Comparison of Experimental and Model-Predicted Data Showing Variation of Pellet Loading with Time at 100°C and 2.45 Mole Per Cent Uranium Hexafluoride.

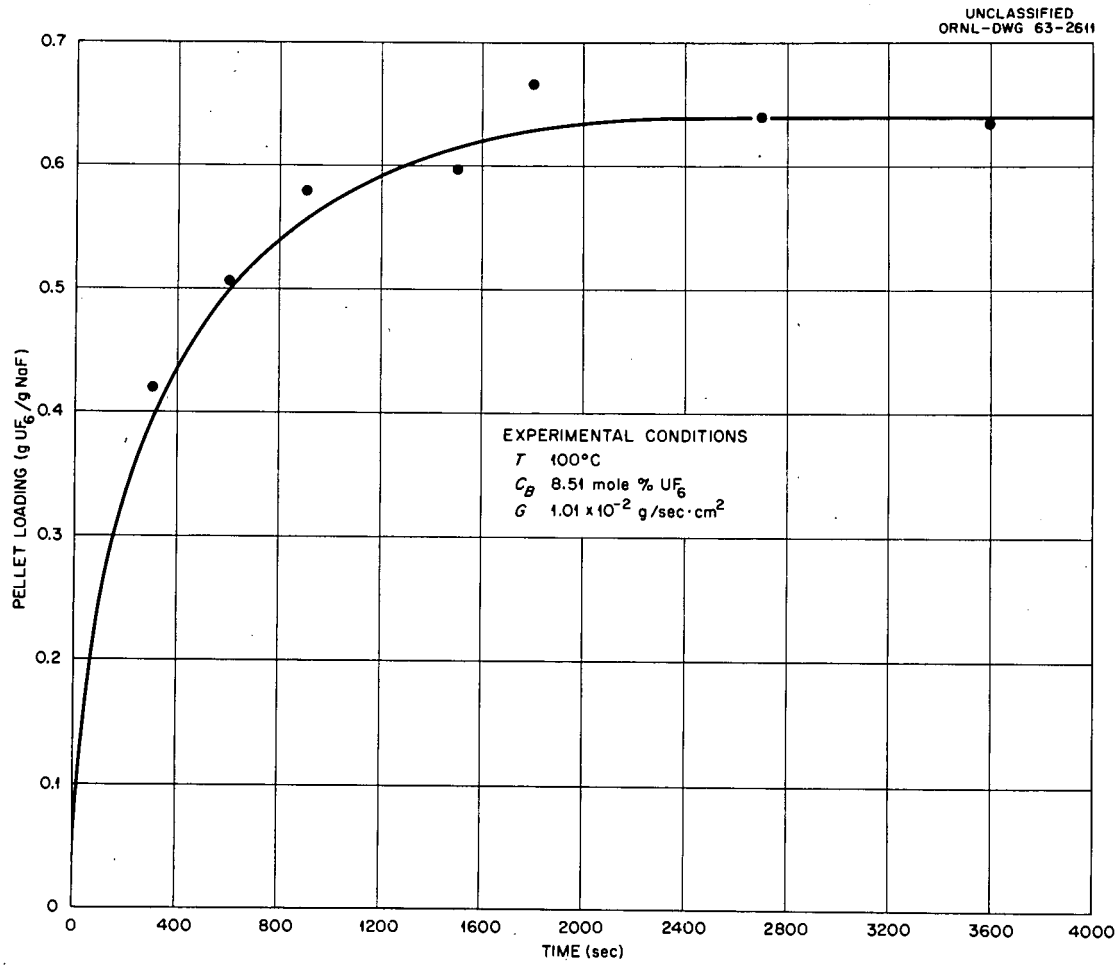

Fig. 3.3 Comparison of Experimental and Model-Predicted Data Showing Variation of Pellet Loading with Time at 100°C and 8.51 Mole Per Cent Uranium Hexafluoride.

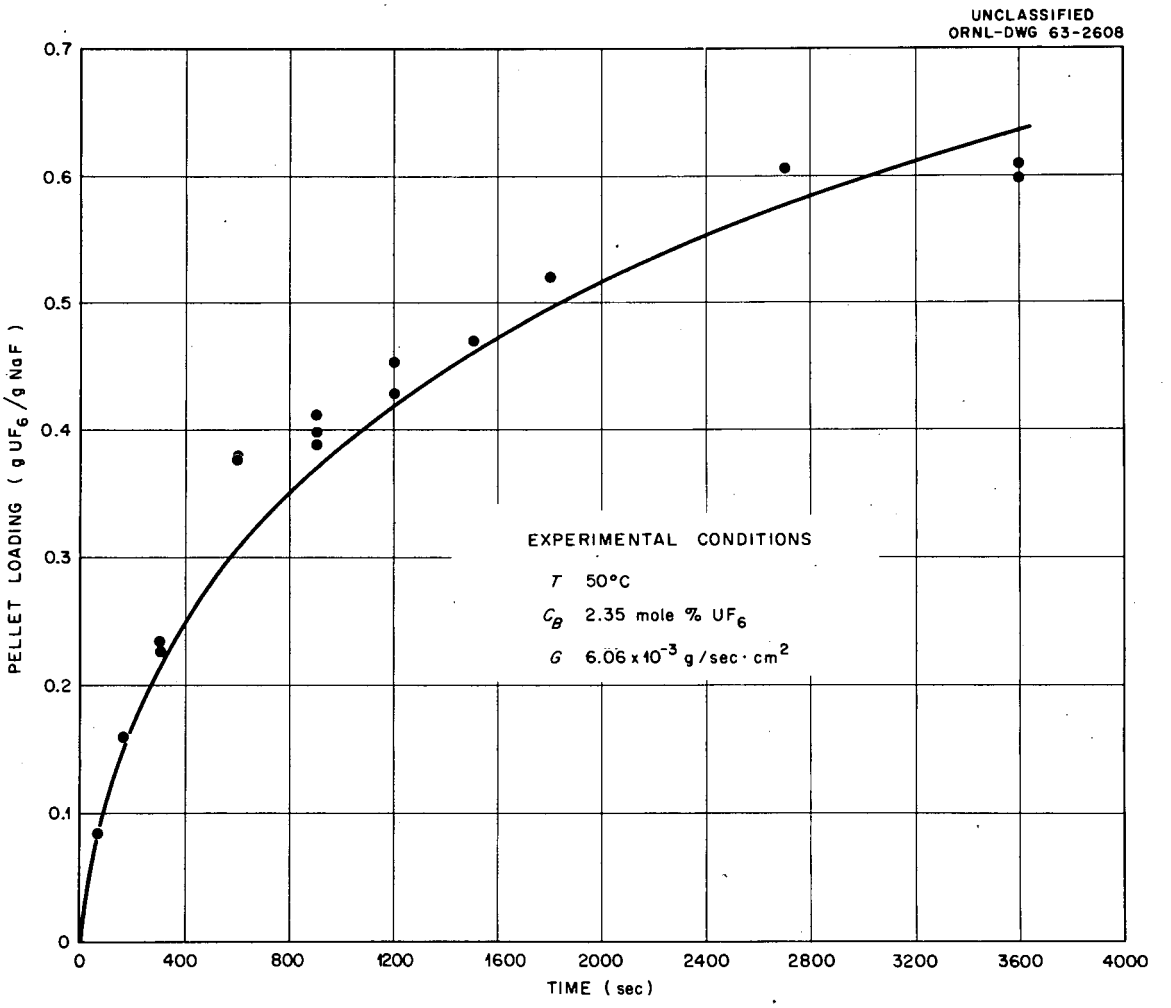

Fig. 3.4 Comparison of Experimental and Model-Predicted Data Showing Variation of Pellet Loading with Time at 50°C and 2.35 Mole Per Cent Uranium Hexafluoride.

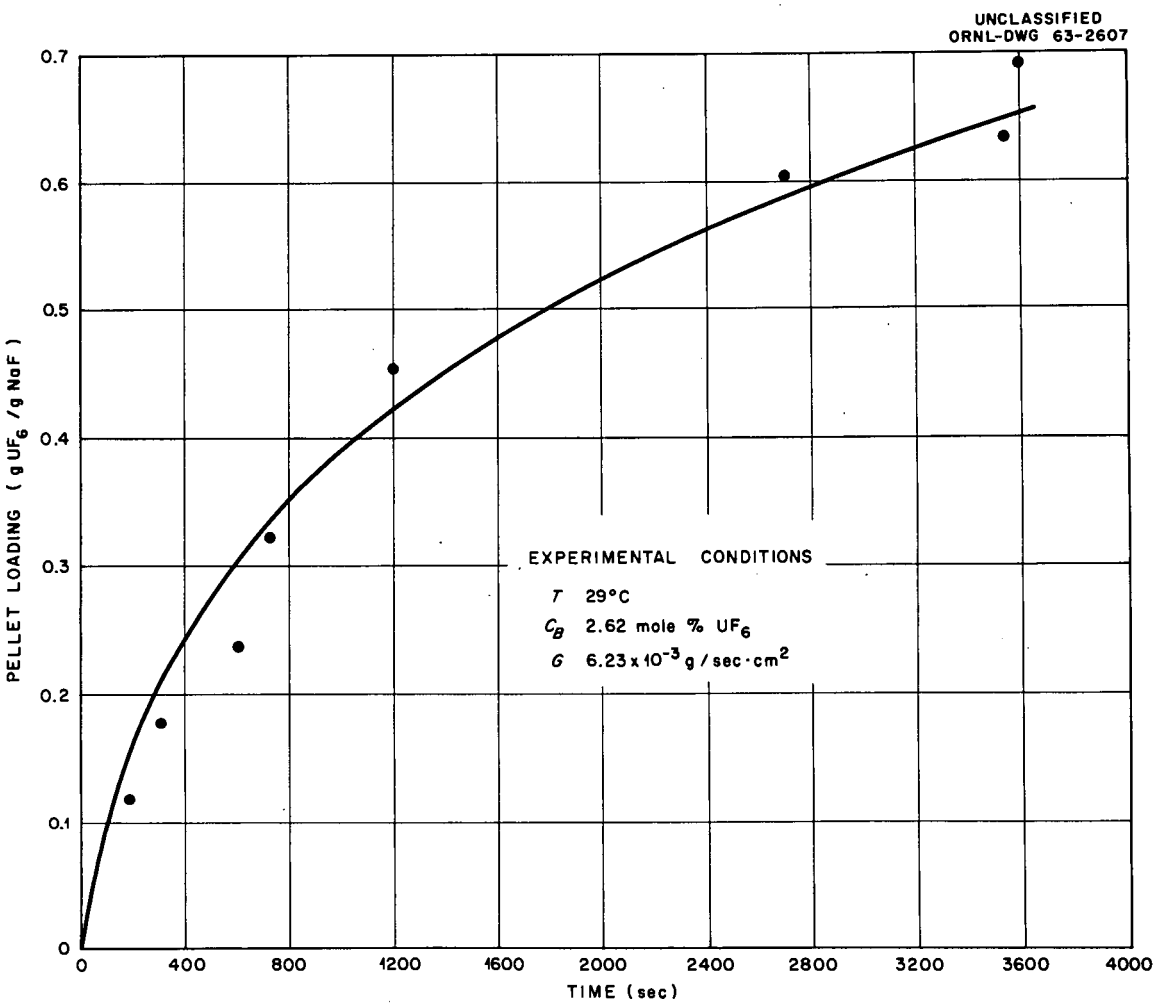

Fig. 3.5 Comparison of Experimental and Model-Predicted Data Showing Variation of Pellet Loading with Time at 29°C and 2.62 Mole Per Cent Uranium Hexafluoride.

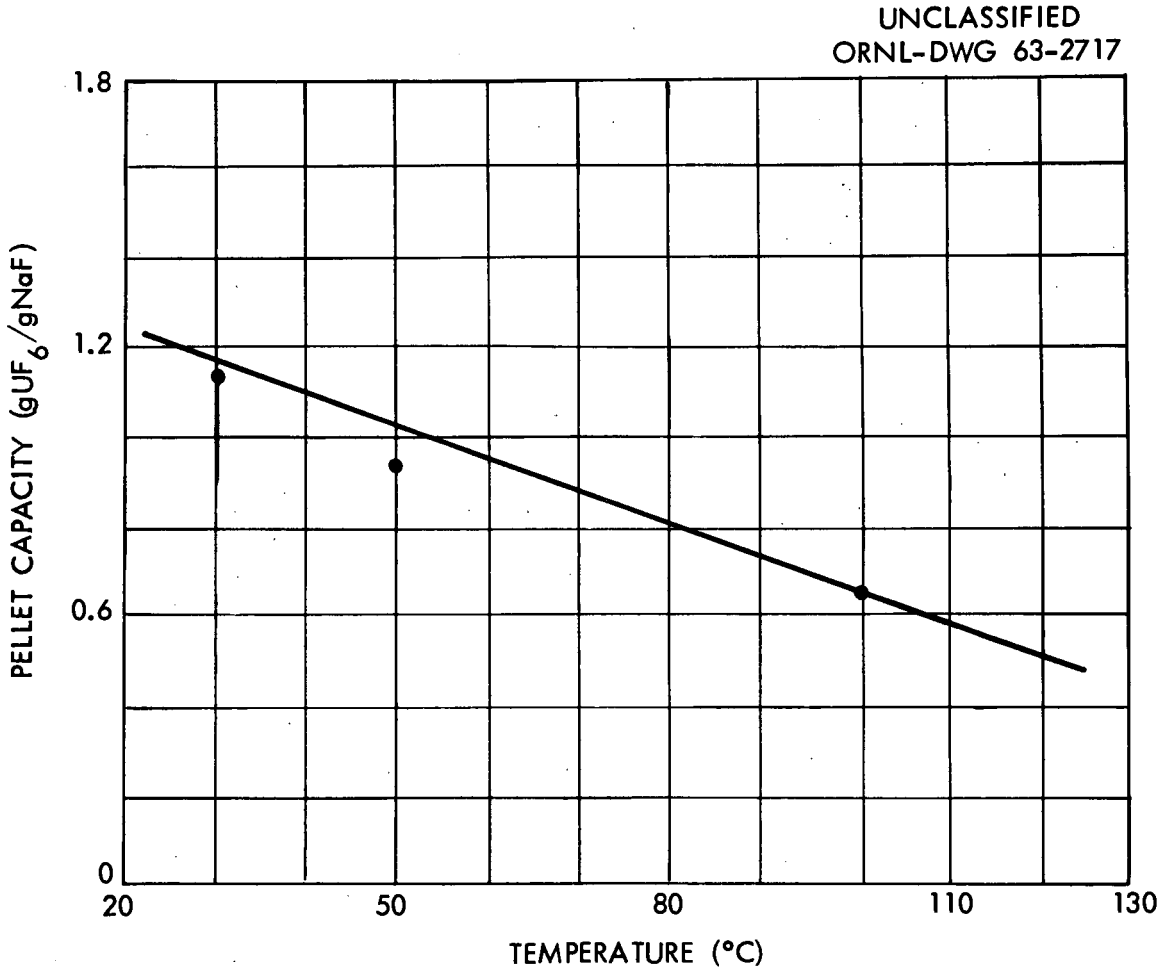

Fig. 3.6 Comparison of Experimentally Determined and Model-Predicted Results on Variation of Effective Pellet Capacity with Temperature.

The effect of a number of pellet properties on sorption rate and capacity have been considered. Thus far, however, the effect of the surface area of the pellet has not been discussed. A dependence of sorption characteristics on surface area is predicted through the dependence of the constants a and b on the surface area. A direct dependence of a on S is predicted and an inverse dependence of b on S. The net result will be a decrease in effective capacity as the surface area is increased. Calculations were made using the computer code for pellets having the same properties as those of the study with the exception of surface area. The results are shown in Fig. 3.7 for the pellets of this study which had a surface area of 0.86 m^2/g and for pellets with surface areas of 1.0 and 1.2 m^2/g. The effective capacity of pellets with a surface area of 1.1 m^2/g is approximately 70% that of pellets having a surface area of 0.86 m^2/g. This result is in agreement with data resulting from repeated use of sodium fluoride pellets. After the first sorption cycle pellets from this study had a surface area of approximately 1.0 m^2/g and an effective capacity of about 65% of the initial capacity.

Application of Data to Sorber Design. The results from the differential-bed studies enable one to predict the rate of removal of uranium hexafluoride from a gas stream by a pellet of sodium fluoride at conditions which may be time dependent; theoretically, one can also use the results to predict the performance of sorber systems such as fixed or moving beds. The calculations necessary for treatment of the general case are somewhat involved and require a finite-difference integration in both time and distance throughout the system. For this reason, the general results will not be included in this report.

One can consider the results for a specific case which is frequently encountered and which will serve to exemplify the effects of the system parameters, temperature, and pellet diameter. The case to be considered is that of a sorber system operating under conditions such that the pellet loading reaches the effective capacity throughout most of the sorber system. Such conditions include sorber systems having low linear gas velocity (0.5 cm/sec in a bed of 10 cm depth) or systems in which the bed occupies an extended length (150 cm at a gas velocity of 5.0 cm/sec). These results, shown in Fig. 3.8, also indicate the minimum quantity of sodium fluoride of the type used in this study which can be expected to sorb a given quantity of uranium hexafluoride and will be useful until more detailed information is available from the general solution.

A topical report (ORNL-3494) was written covering the work summarized in this report.

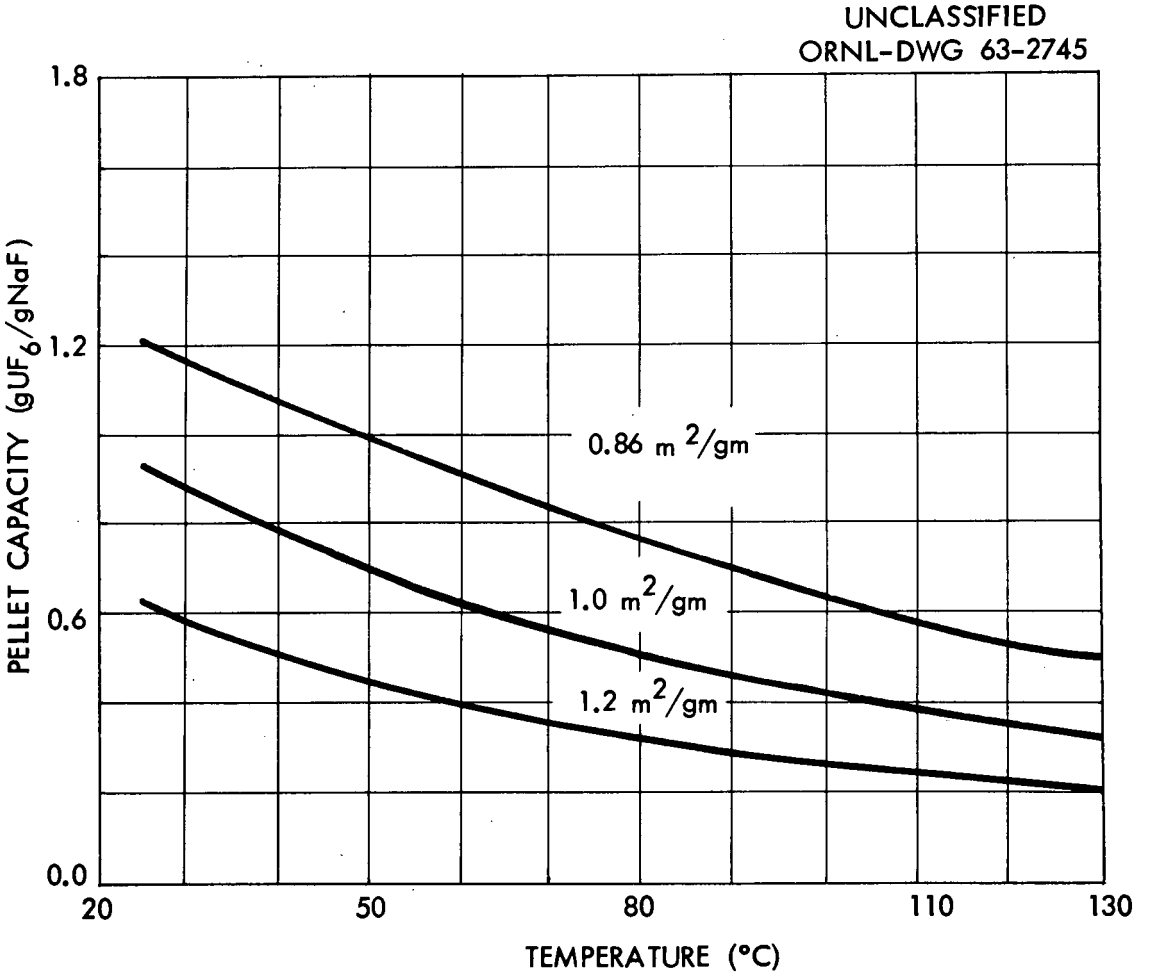

Fig. 3.7 Calculated Values of Effective Pellet Capacity for Pellets having an Initial Void Fraction of 0.45 Showing Effect of Pellet Surface Area.

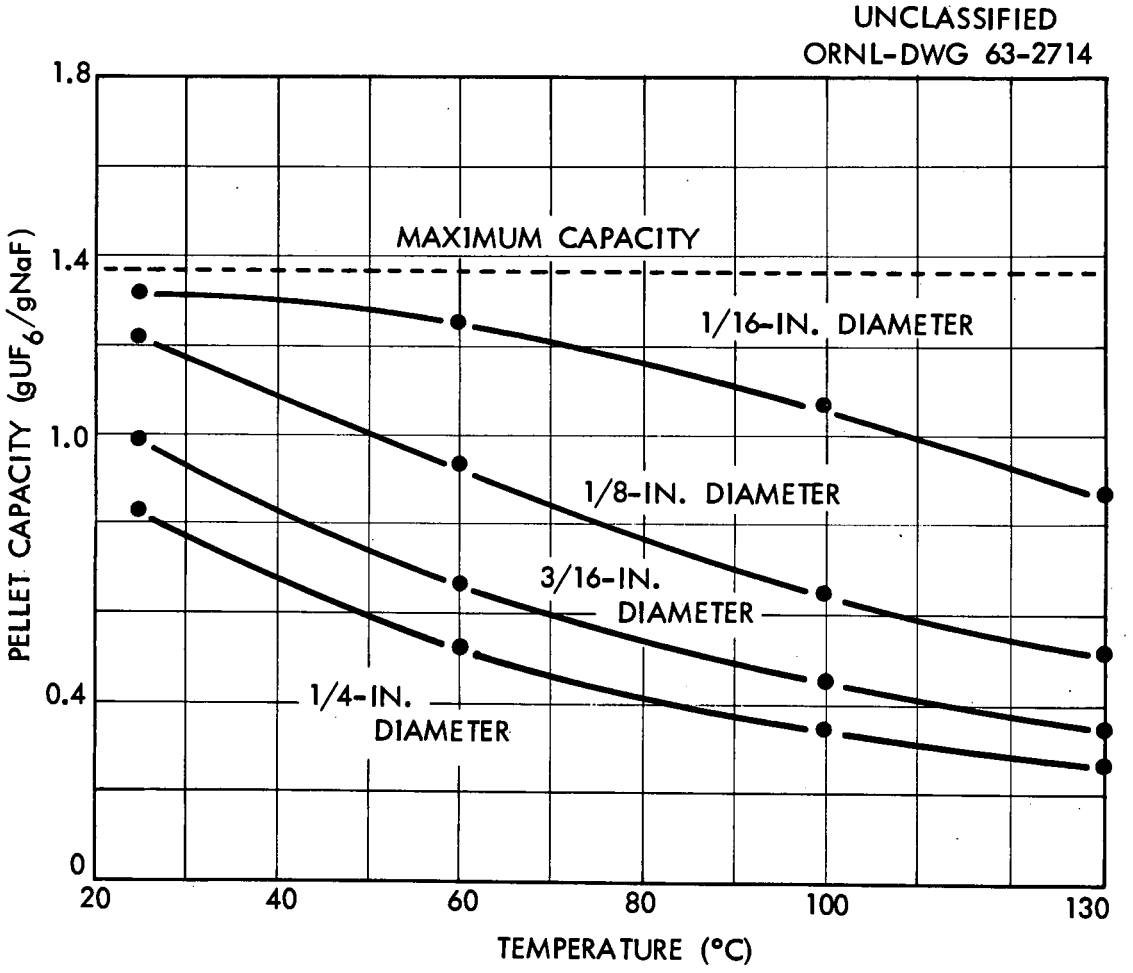

Fig. 3.8 Calculated Values of Effective Pellet Capacity for Pellets having an Initial Void Fraction of 0.45 and a Surface Area of 0.86 Square Meter per Gram.

4.0 WASTE PROCESSING STUDIES

J. C. Suddath

The purpose of waste calcination tests R-77 and R-78 was to test the continuous evaporation and calcination of FTW-65 Purex waste with four times the normal amount of sodium; the normal amount of sodium is 0.3 M, this feed had 1.2 M sodium. In a production plant, an equal amount of sulfate as sulfuric acid would be added so that it would combine to form sodium sulfate, however, for these calcination tests all of the sodium was added as sodium sulfate. The data from these calcination tests are needed for the design of the waste high level pilot plant to be built at Hanford.

4.1 Operating Results and Conclusions for Tests R-77 and R-78 - C. W. Hancher

Tests R-77 and R-78 were exact duplicate tests using continuous evaporation. The feed for these tests was FTW-65 Purex with four times the normal amount of sodium (Table 4.1). The normal amount of sodium is 0.3 M, this feed was made up to 1.2 M sodium using sodium sulfate (0.6 M sulfate). Calcium nitrate was added continuously during the calciner feeding period so that the calcium molar content in the calciner would be 10% of the total sulfate in the calciner.

The maximum feed rate during test R-77 was 72 liters/hr, the average feed rate was 18.6 liters/hr (Table 4.2). The average feed rate for test R-78 was 19.2 liters/hr with a maximum of 132 liters/hr (Table 4.3). The total amount of feed used during these two tests was 726 and 904 liters, respectively. The bulk densities of the solids were 1.26 and 1.36 g/cc, respectively, which reflect the difference in the amount of feed used. The residual nitrate in the solid was 100 ppm for R-77 and 140 ppm for R-78.

The material balance for test R-77 (Table 4.4) showed an incomplete balance for nitrate and more than 100% for the other constituents, however, these balances appear to be within the sampling and analytical error. The material balance for R-78 (Table 4.5) is acceptable except for nitrate which was a 154% balance.

The entrainment and volatilization of components into the calciner condensate are shown in Table 4.6. The relative sulfate concentration in the calciner condensate for test R-77 is less than iron and sodium, therefore, it is inferred that all of the sulfate was carry over associated with iron and sodium and none of it was due to volatility. The same can be said for test R-78. The entrainment is high because this feed composition tended to foam a great deal. One of the contributing reasons for the high amount of entrainment for test R-78 was that the liquid level was operated about 5 in. higher than normal due to the misplacement of the calciner liquid level probe. There also apparently was a partial plug in the top of the calciner during the early phase of test R-78 which further increased entrainment into the calciner off-gas line.

Table 4.1. Feed and Solid Composition for Tests R-77 and R-78

	NO_3	Fe	Na	Hg	SO_4
Feed					
R-77 (g/liter)	137	10.2	27.3	0.90	60.8
(M)	2.2	0.19	1.19	0.0045	0.63
R-78 (g/liter)	117	6.0	27.3	1.7	62.2
(M)	1.86	0.11	1.19	0.0085	0.65
Solid (wt %)					
R-77	0.01	8.85	23.6	3.04	55.7
Bulk density	1.26 g/cc				
R-78	0.014	3.55	28.0	3.08	59.6
Bulk density	1.36 g/cc				

Table 4.2 Hourly System Variables and Parameters

TEST R- 77 FEED TYPE - FTW-65 (SULFATE) OPERATION MODE - CONTINUOUS

RUN TIME HOURS	SYSTEM FEED LITERS	SYSTEM WATER LITERS	CALCINER ADDITIVE LITERS	EVAPORATOR CONDENSATE LITERS	CALCINER FURNACE (HUNDRED-THOUSANDS OF BTUS)	CALCINER CONDENSATE	EVAPORATOR CONDENSATE	SYSTEM OFF-GAS CU FT	EVAPORATOR DENSITY GM/CC	CALCINER CONDENSATE LITERS
1	88			37	1.30	.01	1.98	12	1.03	1
2	104	31	2	69	2.60	.05	3.69	23	1.20	2
3	140	30	2	105	3.88	.73	5.11	34	1.23	31
4	153	30	2	119	5.16	1.68	6.16	46	1.22	70
5	220	31	4	189	6.45	2.61	7.80	57	1.23	108
6	254	31	5	223	7.73	3.56	9.63	68	1.29	146
7	296	32	6	267	8.97	4.52	10.87	79	1.30	186
8	335	28	7	302	10.13	5.35	12.09	91	1.29	220
9	356	58	7	355	11.28	6.17	13.57	102	1.29	254
10	384	58	8	383	12.40	6.95	14.82	113	1.29	286
11	421	59	8	420	13.47	7.69	16.04	126	1.28	318
12	478	115	10	534	14.51	8.40	19.47	139	1.25	349
13	496	115	11	555	15.49	8.98	20.67	152	1.31	374
14	532	142	11	618	16.36	9.46	21.93	166	1.27	395
15	557	142	12	642	17.07	9.87	23.65	180	1.27	413
16	570	141	12	654	17.69	10.19	24.82	193	1.29	428
17	592	172	12	708	18.20	10.47	25.92	207	1.29	440
18	623	172	13	739	18.69	10.69	26.98	220	1.29	450
19	629	172	13	745	19.13	10.87	28.00	234	1.29	459
20	628	173	13	747	19.51	10.99	28.79	249	1.30	464
21	635	199	13	778	19.90	11.15	29.82	262	1.28	471
22	667	199	14	809	20.27	11.26	30.80	275	1.30	476
23	667	199	14	811	20.62	11.35	31.37	289	1.30	480
24	667	226	14	839	20.98	11.44	32.23	302	1.29	484
25	671	225	14	841	21.32	11.52	33.17	315	1.29	488
26	677	254	14	874	21.66	11.62	34.13	327	1.27	493
27	679	256	14	876	21.99	11.70	34.83	339	1.29	496
28	679	255	14	878	22.30	11.78	35.48	351	1.29	500
29	695	255	14	891	22.62	11.84	36.09	363	1.30	502
30	693	282	14	915	22.91	11.86	36.58	376	1.33	504
31	696	282	14	914	23.23	11.98	37.06	387	1.34	509
32	692	281	14	907	23.53	12.03	37.51	399	1.37	511
33	696	282	14	915	23.81	12.05	37.67	413	1.37	512
34	692	282	14	908	24.08	12.05	37.80	427	1.55	512
35	696	312	14	936	24.41	12.30	38.37	439	1.15	523
36	699	312	14	957	24.86	12.58	39.89	450	1.20	536
37	696	485	14	1126	25.28	12.78	43.66	462	1.20	545
38	754	601	15	1300	25.65	12.90	48.28	473	1.15	551
39	756	632	14	1327	25.97	12.95	49.10	486	1.21	553
40	760	632	14	1337	26.25	12.96	49.79	499	1.32	553
41	760	659	14	1365	26.54	12.99	50.32	513	1.38	555
42	764	659	15	1367	26.81	12.99	50.83	528	1.35	555
43	761	659	14	1363	27.07	12.99	51.35	542	1.31	555
44	763	659	14	1363	27.32	12.99	51.84	557	1.29	555
45	764	689	14	1394	27.56	12.99	52.34	572	1.29	555
46	764	689	14	1395	27.79	12.99	52.93	586	1.29	555
47	763	689	15	1396	28.02	12.99	53.49	600	1.30	555
48	781	689	18	1411	28.27	13.03	54.08	613	1.31	556
49	781	690	18	1421	28.55	13.04	54.79	626	1.37	557
50	780	716	18	1445	28.80	13.04	55.32	639	1.45	557
51	780	716	18	1445	29.06	13.11	55.82	651	1.40	560
52	783	716	18	1448	29.34	13.20	56.44	662	1.35	564
53	783	745	18	1478	29.63	13.29	57.13	675	1.24	568
54	780	746	18	1475	29.92	13.36	57.79	687	1.25	571
55	780	773	18	1501	30.20	13.42	58.43	698	1.23	573
56	779	772	18	1501	30.47	13.43	59.06	710	1.28	574
57	780	799	18	1531	30.73	13.43	59.70	723	1.30	574
58	785	798	19	1537	30.97	13.43	60.34	737	1.30	574
***TAPE PARITY ERROR NEXT LINE										
59	780	799	18	15134	31.20	13.43	61.00	751	1.30	574
60	783	829	18	1567	31.39	13.43	61.65	764	1.31	574
61	780	829	18	1563	31.62	13.43	62.34	776	1.33	574
62	781	855	18	1589	31.84	13.43	63.03	789	1.18	574
63	780	856	18	1589	32.07	13.43	63.72	802	1.18	574

Table 4.3 Hourly System Variables and Parameters

TEST R- 78 FEED TYPE - FTW-65 (SULFATE) OPERATION MODE - CONTINUOUS

RUN TIME	SYSTEM FEED	SYSTEM WATER	CALCINER ADDITIVE	EVAPORATOR CONDENSATE	CALCINER FURNACE	CALCINER CONDENSATE	EVAPORATOR CONDENSATE	SYSTEM OFF-GAS	EVAPORATOR DENSITY	CALCINER CONDENSATE
HOURS	LITERS	LITERS	LITERS	LITERS	(HUNDRED-THOUSANDS OF BTUS)			CU FT	GM/CC	LITERS
1	36	27		29	1.03	.00	2.08	12	1.12	
2	161	27	3	136	2.28	.86	5.46	24	1.20	34
3	238	85	5	281	3.52	1.63	8.35	35	1.35	67
4	351	85	8	387	4.77	2.55	12.80	46	1.32	104
5	466	110	10	542	5.98	3.25	16.35	57	1.29	134
6	510	141	11	605	7.03	3.80	18.94	70	1.36	157
7	567	165	12	687	7.98	4.29	21.05	82	1.32	178
8	599	192	12	747	8.79	4.70	23.08	96	1.31	196
9	632	219	12	806	9.46	5.05	24.93	109	1.31	212
10	704	246	12	906	10.05	5.32	27.17	122	1.29	224
11	722	245	12	924	10.56	5.55	28.43	135	1.39	234
12	753	276	12	986	11.03	5.74	29.61	148	1.33	243
13	755	303	13	1011	11.55	5.98	30.63	162	1.37	254
14	761	301	18	1020	12.07	6.31	31.39	175	1.37	269
15	766	328	17	1056	12.62	6.67	32.26	188	1.33	285
16	768	327	17	1054	13.17	7.03	32.94	200	1.52	301
17	770	355	17	1088	13.74	7.41	33.97	214	1.30	319
18	790	355	17	1115	14.34	7.83	35.28	226	1.30	337
19	793	412	17	1169	14.82	8.03	37.88	239	1.41	346
20	793	438	17	1197	15.19	8.12	38.75	253	1.38	351
21	796	439	17	1197	15.61	8.47	39.49	267	1.33	367
22	797	465	17	1224	16.13	8.83	40.23	279	1.33	382
23	795	465	17	1216	16.67	9.16	40.88	292	1.35	398
24	795	465	17	1223	17.21	9.49	41.98	304	1.31	412
25	804	491	17	1256	17.71	9.79	42.95	316	1.32	426
26	808	492	17	1260	18.28	10.08	43.93	330	1.31	439
27	808	492	17	1260	18.68	10.36	44.68	343	1.32	452
28	812	520	17	1289	19.12	10.49	45.47	356	1.31	458
29	809	521	17	1285	19.47	10.58	46.17	370	1.29	461
30	809	822	17	1291	19.83	10.69	46.93	384	1.30	467
31	808	547	17	1315	20.16	10.73	47.69	398	1.29	469
32	809	547	17	1317	20.46	10.75	48.46	414	1.25	469
33	811	545	17	1319	20.74	10.75	49.16	429	1.30	469
34	809	576	17	1348	21.01	10.75	49.89	444	1.30	469
35	813	576	17	1352	21.26	10.75	50.53	459	1.31	469
36	813	576	17	1354	21.50	10.75	51.16	474	1.32	469
37	808	603	17	1376	21.74	10.75	51.77	488	1.33	469
38	808	603	17	1377	21.97	10.75	52.38	503	1.36	469
39	811	629	17	1405	22.21	10.75	53.37	516	1.31	469
40	813	686	17	1463	22.42	10.75	54.78	530	1.30	469
41	813	743	17	1520	22.64	10.75	56.56	544	1.29	469
42	811	826	17	1602	22.86	10.75	58.66	558	1.29	469
43	825	880	17	1666	23.10	10.81	61.24	572	1.26	472
44	852	879	19	1688	23.47	11.02	62.24	584	1.31	482
45	853	905	19	1719	23.87	11.21	62.89	596	1.26	490
46	854	905	19	1726	24.26	11.34	63.61	610	1.28	496
47	854	905	19	1714	24.62	11.52	63.87	622	1.30	504
48	854	936	19	1754	25.01	11.69	65.09	636	1.22	512
49	854	962	19	1784	25.35	11.77	66.01	650	1.37	516
50	852	1015	19	1832	25.68	11.85	67.38	663	1.24	519
51	853	1040	19	1859	25.98	11.88	68.85	676	1.21	521
52	853	1093	19	1913	26.25	11.89	70.07	691	1.22	521
53	852	1124	19	1938	26.51	11.95	71.28	703	1.13	524
54	850	1178	19	1992	26.77	11.99	72.52	717	1.10	526
55	852	1235	19	2050	27.03	12.02	73.94	730	1.07	527
56	850	1262	19	2077	27.28	12.13	75.47	743	1.15	532
57	853	1289	19	2107	27.53	12.22	76.47	757	1.14	536
58	855	1315	19	2134	27.75	12.30	77.54	770	1.13	540
59	853	1341	19	2159	27.97	12.37	78.59	783	1.13	543
60	850	1373	19	2187	28.20	12.43	79.61	797	1.13	545
61	854	1399	19	2218	28.42	12.49	80.61	811	1.13	548
62	851	1454	19	2269	28.63	12.54	81.66	825	1.13	550
63	850	1479	19	2294	28.85	12.60	82.81	838	1.12	553
64	855	1509	19	2328	29.06	12.66	84.01	852	1.12	555
65	851	1566	19	2381	29.26	12.71	85.22	865	1.11	557
66	858	1593	19	2415	29.47	12.76	86.55	879	1.11	559
67	852	1650	19	2466	29.67	12.81	87.81	892	1.09	562
68	851	1677	19	2492	29.88	12.86	89.17	904	1.07	564
69	852	1734	19	2549	30.08	12.91	90.62	917	1.06	566
70	854	1790	19	2608	30.28	12.92	92.10	931	1.06	566
71	855	1848	19	2666	30.48	12.94	93.64	944	1.05	567
72	852	1901	19	2716	30.69	12.95	95.13	957	1.05	568
73	851	1958	19	2772	30.89	12.97	96.71	971	1.05	568
74	853	2011	19	2827	31.10	12.98	98.33	984	1.05	569
75	852	2073	19	2888	31.29	12.98	100.05	997	1.04	569
76	855	2130	19	2948	31.49	12.98	101.83	1010	1.04	569

Table 4.4. Material Balance for Test R-77

	NO_3	Fe	Na	Hg	SO_4
IN: (wt in g)					
Feed	99,462	7,260	19,819	653	44,286
OUT:					
Evaporator	6,415	470	1,137	72	2,608
Evaporator Condensate	79,168	1	2	32	32
Solid	7	7,752	20,748	684	46,208
Total	85,592	8,223	21,886	788	48,848
Balance (%)	86.1	113.3	110.4	120.6	110.3

Table 4.5. Material Balance for Test R-78

	NO_3	Fe	Na	Hg	SO_4
IN: (wt in g)					
Feed	105,768	5,424	24,589	1,564	56,138
OUT:					
Evaporator	6,450	325	1,387	243	3,275
Evaporator Condensate	156,831	1	1	45	30
Solid	12	3,013	23,769	2,614	50,594
Total	163,283	3,338	25,157	2,902	53,899
Balance (%)	154.4	61.5	102.3	185.5	96.01

Table 4.6. Entrainment and Volatilization of Components Into Calciner Condensate

(% of Total Feed to System)

	NO_3	Fe	Na	Hg	SO_4
R-77	182	00.27	0.13	110	0.07
R-78	157	27[a]	30[a]	151	26[a]

[a]R-78 Fe, Na, SO_4 are high because of a foam-over of raw feed.

4.2 Operating Control and Temperature Profiles for Tests R-77 and R-78

Graphical representations for the control variables for the calciner liquid level, evaporator liquid level, evaporator density, evaporator vapor conductivity, and evaporator vapor pressure for test R-77 are shown in Figs. 4.1 through 4.5 and for test R-78 are shown in Figs. 4.6 through 4.10.

The calciner liquid level control, Figs. 4.1 and 4.6, for the two tests indicate 0% control scale when the calciner was over-filled and 100% of control scale when the calciner was under-filled. The control scale range indicates about 4 in. of liquid level. The initial over-filling was worse in R-78 than in R-77, however, this is partially due to the misplaced liquid level probe which was 5 in. high in R-78.

The evaporator liquid level control for the two tests, Figs. 4.2 and 4.7, show a satisfactory controlled condition during most of the test. The control scale for this parameter is about 14 liters at 0% of the scale and 44 liters at 100% of the scale, however, it is not serious if liquid is accumulated to greater than 100% of the scale. The fluctuation in test R-78 was due to the liquid level lines plugging and being flushed with water to free them.

The density control for the two tests are shown in Figs. 4.3 and 4.8. The density control for R-77 was good but slightly higher than the predetermined set point; this is not serious. The control of R-78 density was satisfactory except the density lines became partially plugged several times. Peaks show cleaning of the plugged lines.

The evaporator vapor conductivity is a very unpredictable variable but is not of high significance. The control of this variable is acceptable for both tests. The evaporator vapor pressure control for both tests was good.

The temperature profiles for test R-77 are shown in Figs. 4.11 through 4.18. Figure 4.12 shows the upper thermocouple of the calciner vessel, the sudden drop in temperatures are due to the addition of liquid feed in the top part of the calciner during a period of time when the thermocouples were in excess of 400°C. Temperature profiles for test R-78 are shown in Figs. 4.19 through 4.26. The sudden variation of temperatures in Figs. 4.19 and 4.21 is caused by the addition of liquid feed to the hot calciner vessel during various times during the test.

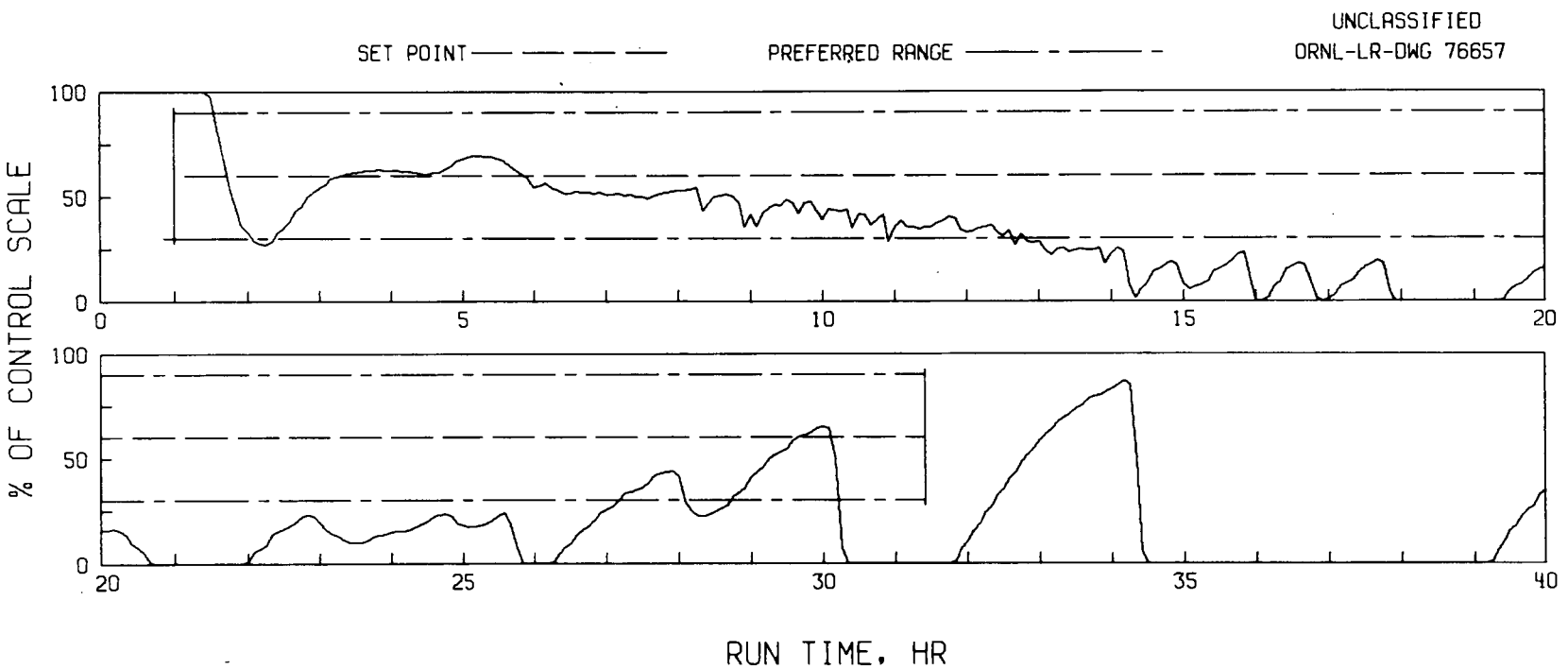

Fig. 4.1 Calciner Liquid Level Controller. Waste Calcination Test 77. Continuous Evaporation. Purex FTW-65.

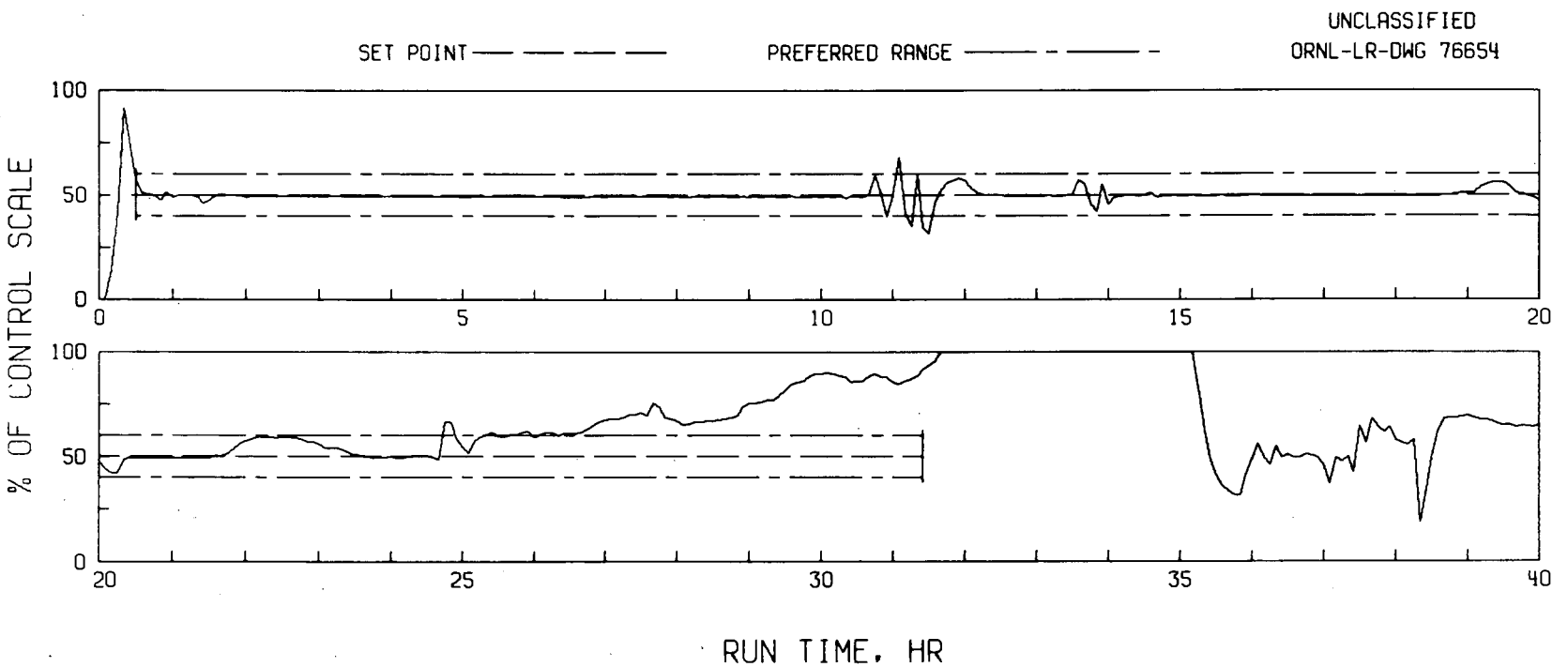

Fig. 4.2 Evaporator Liquid Level Controller. Waste Calcination Test 77. Continuous Evaporation. Pures FTW-65.

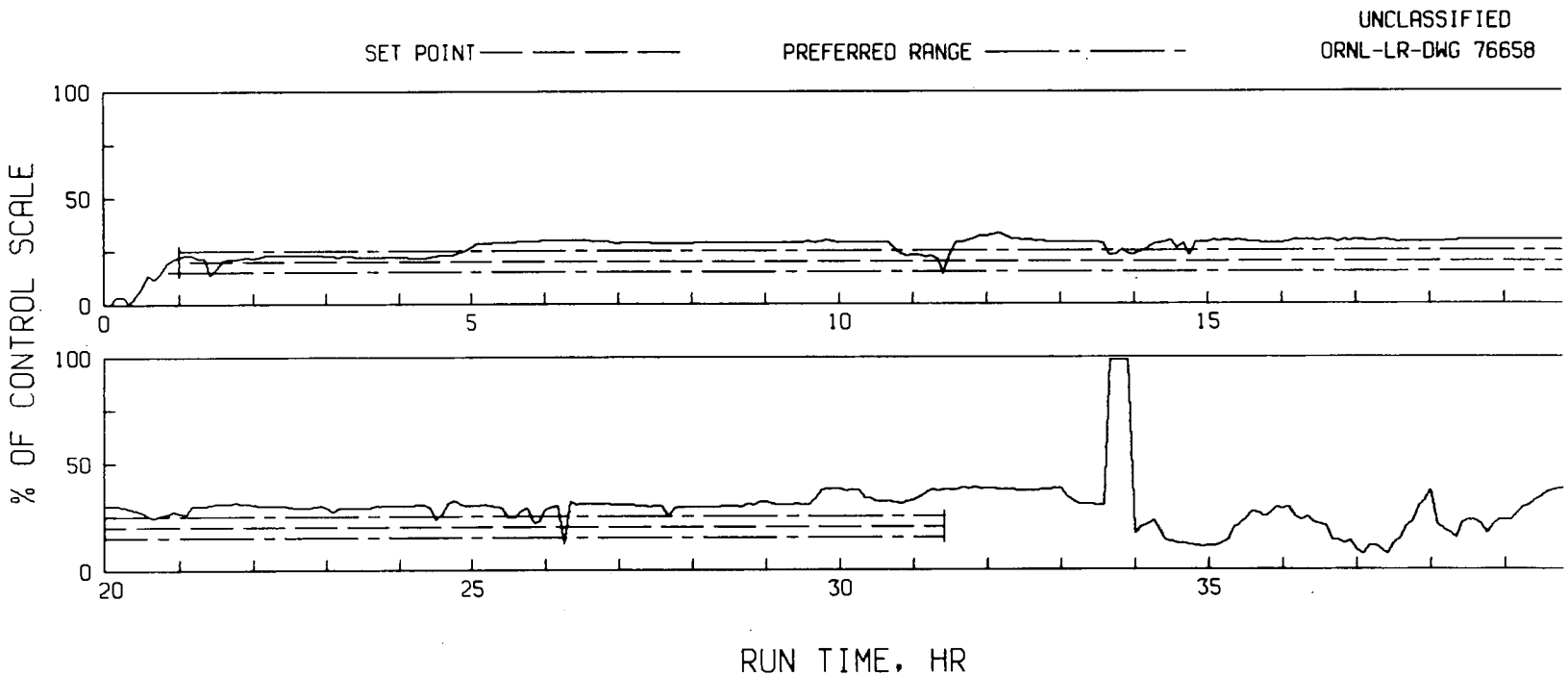

Fig. 4.3 Evaporator Density Controller. Waste Calcination Test 77. Continuous Evaporation. Purex FTW-65.

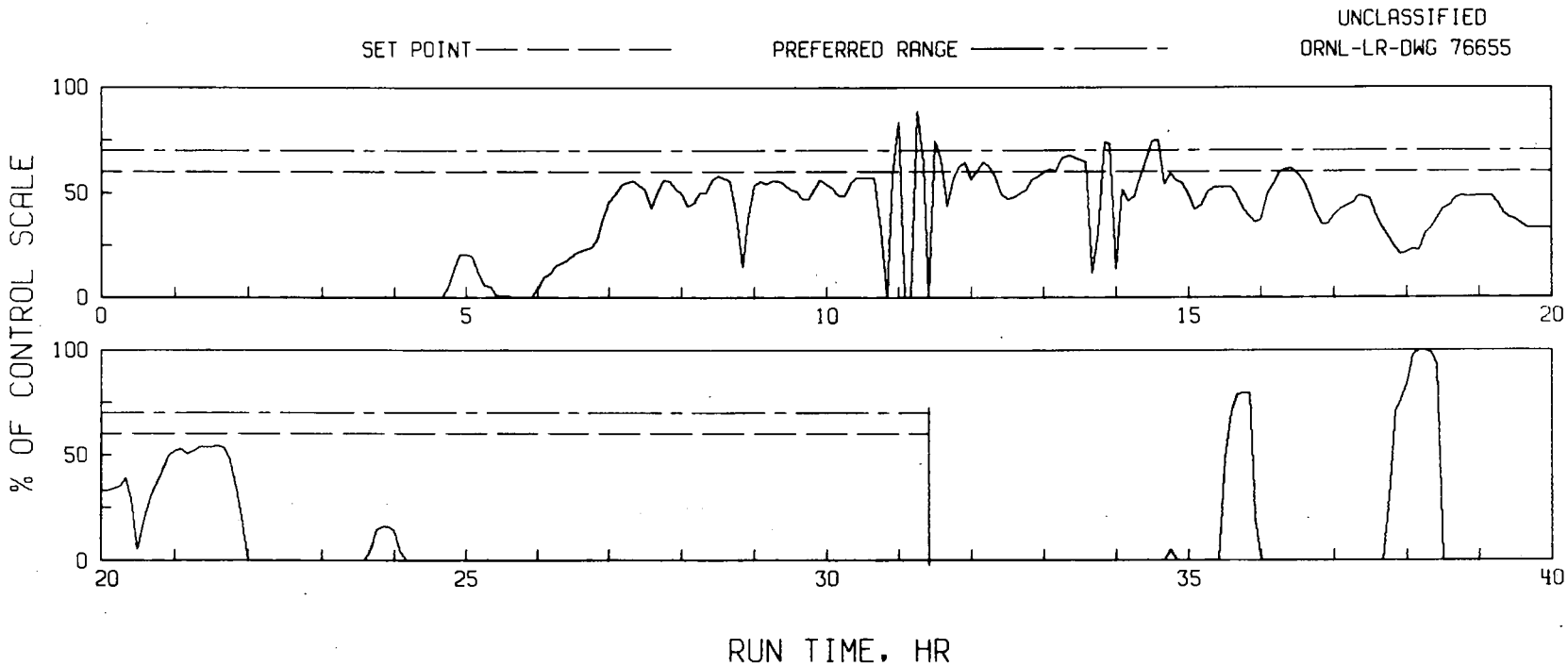

Fig. 4.4 Evaporator Vapor Conductivity Controller. Waste Calcination Test 77. Continuous Evaporation. Purex FTW-65.

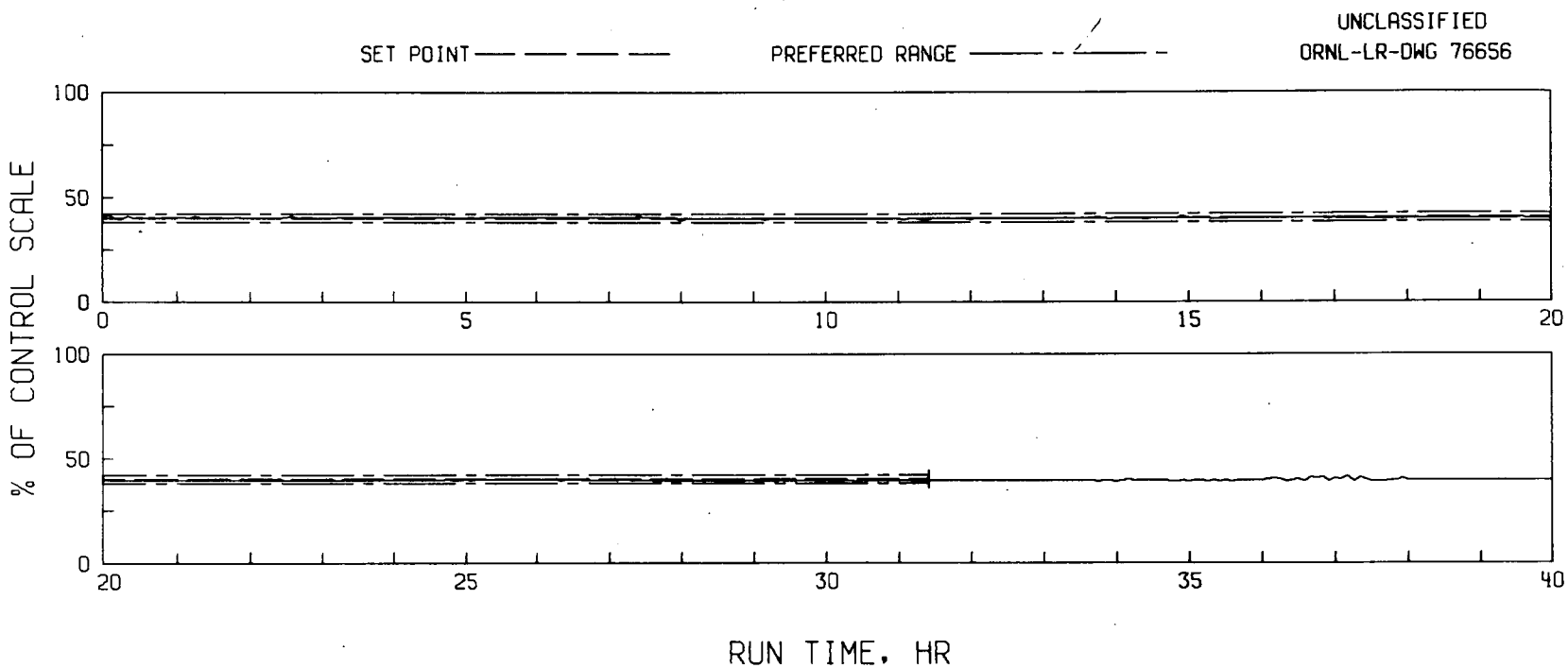

Fig. 4.5 Evaporator Vapor Pressure Controller. Waste Calcination Test 77. Continuous Evaporation. Purex FTW-65.

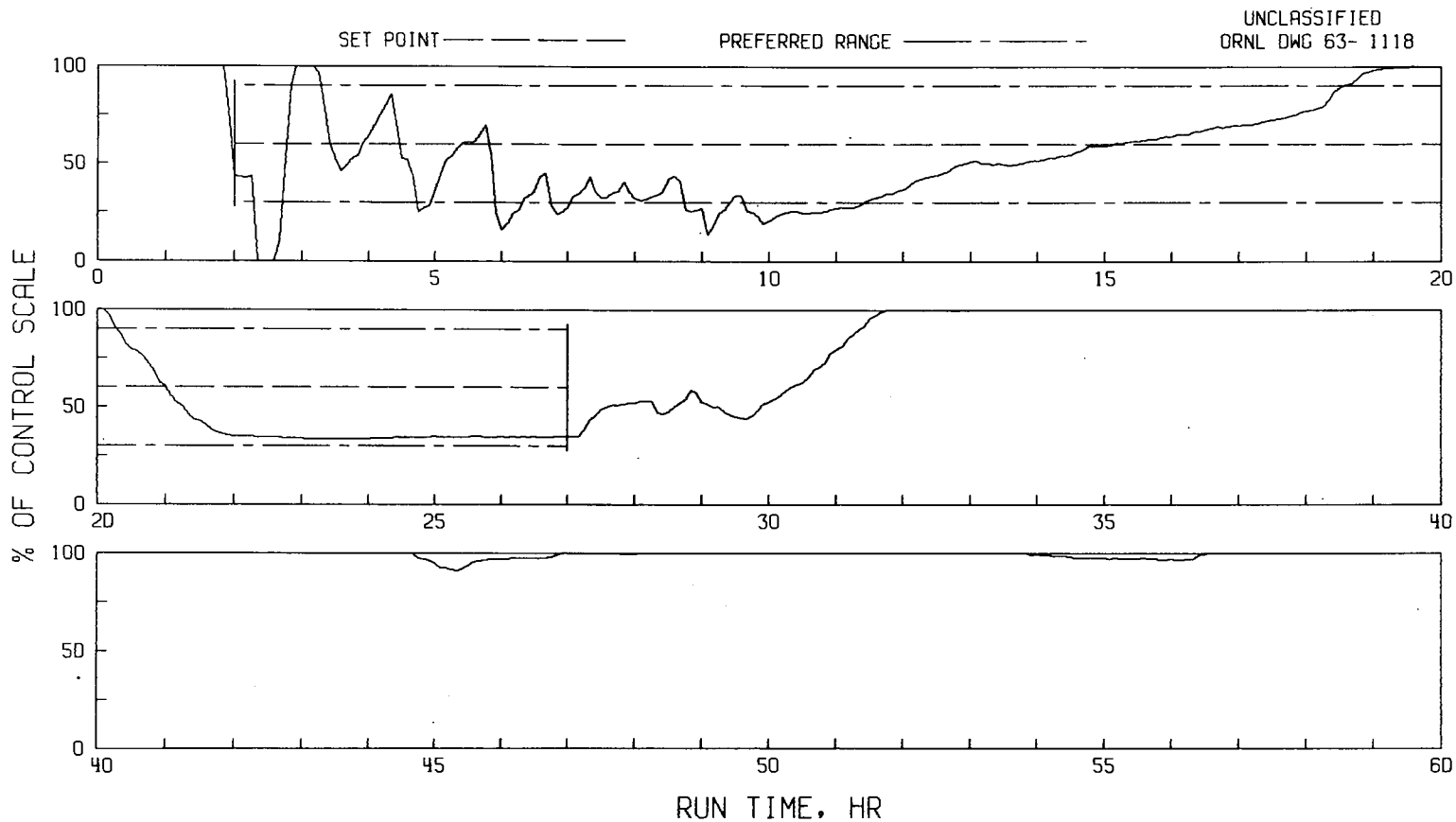

Fig. 4.6 Calciner Liquid Level Controller. Waste Calcination Test 78. Continuous Evaporation. Purex FTW-65.

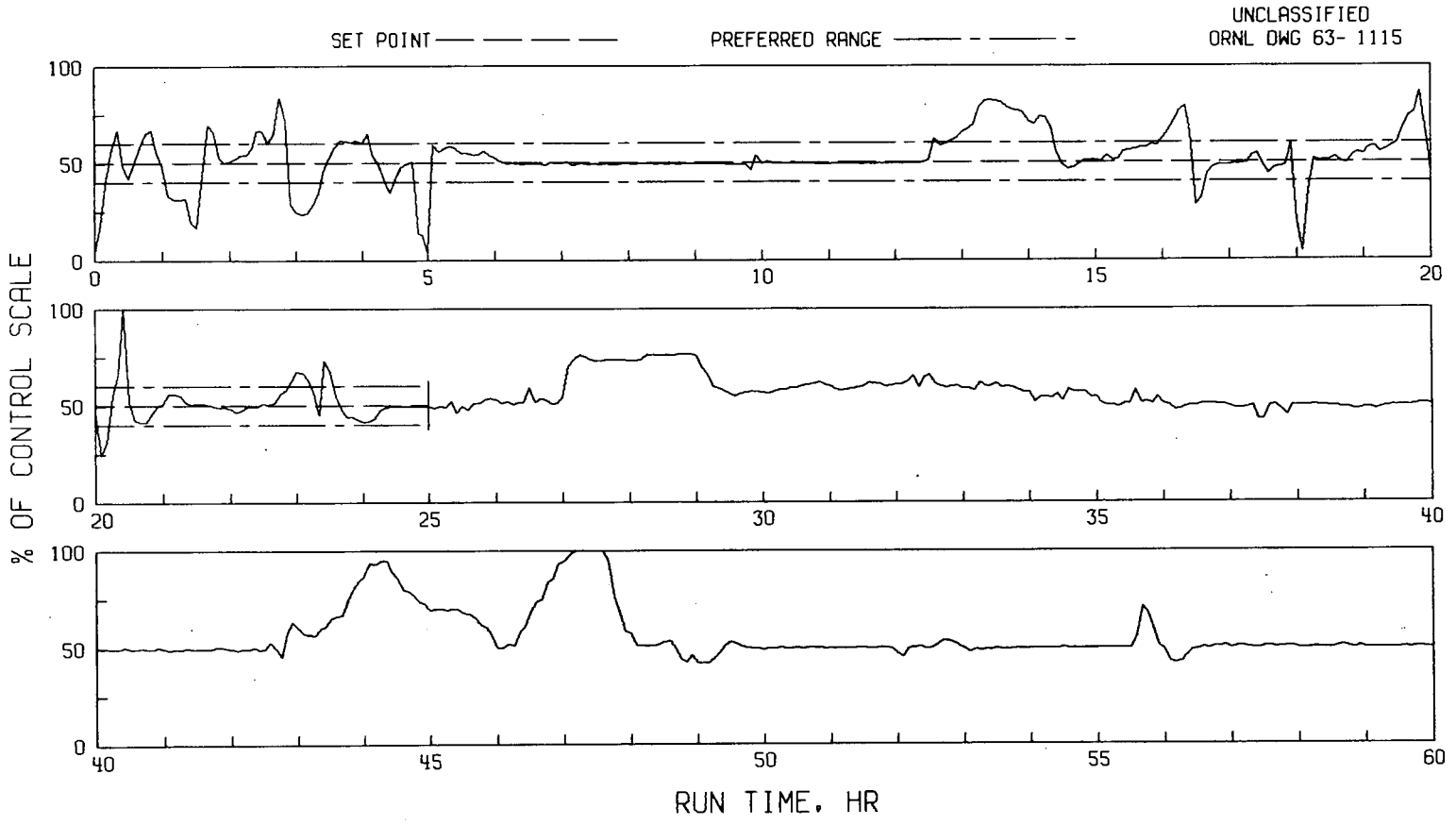

Fig. 4.7 Evaporator Liquid Level Controller. Waste Calcination Test 78. Continuous Evaporation. Purex FTW-65.

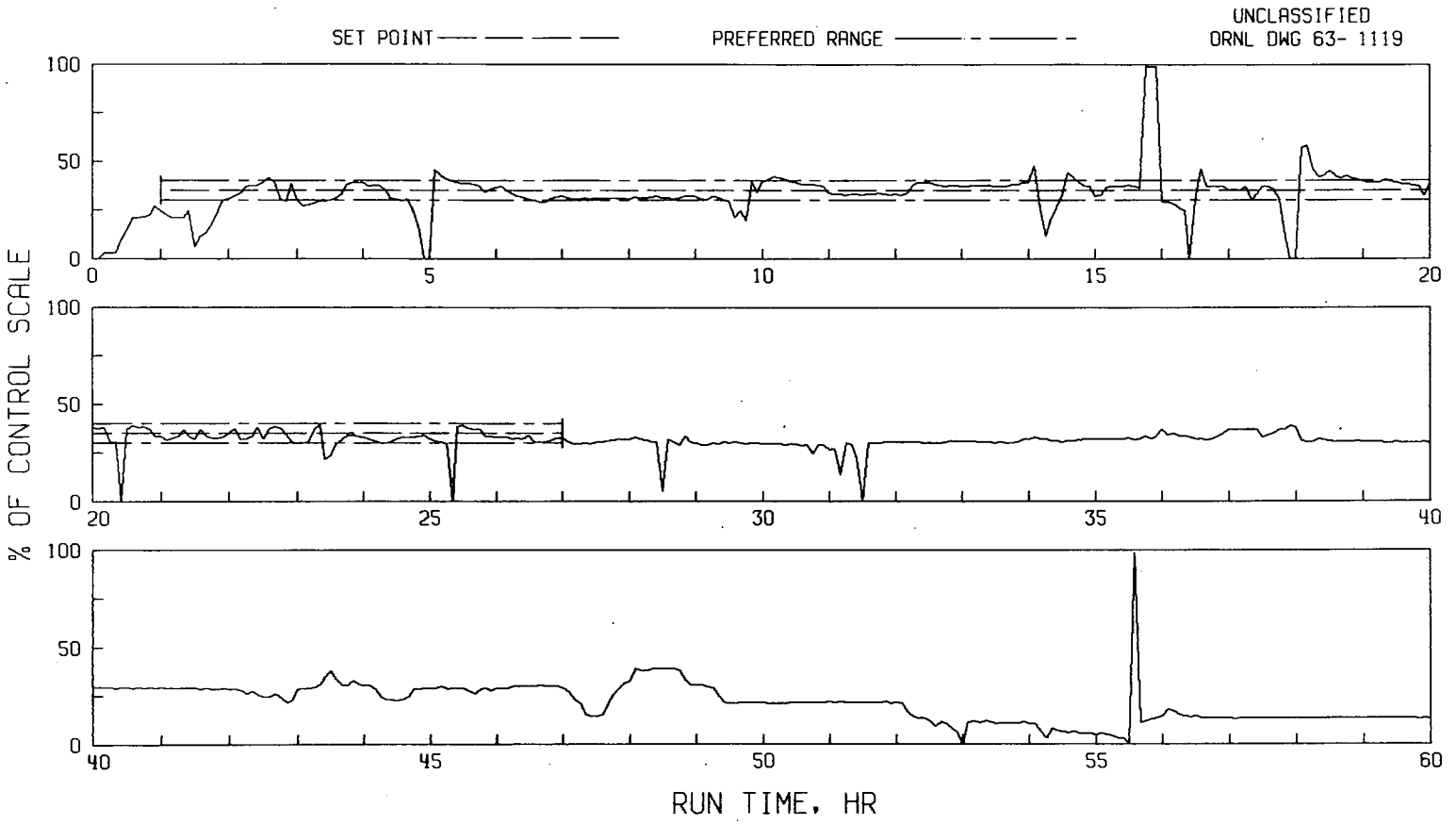

Fig. 4.8 Evaporator Density Controller. Waste Calcination Test 78. Continuous Evaporation. Purex FTW-65.

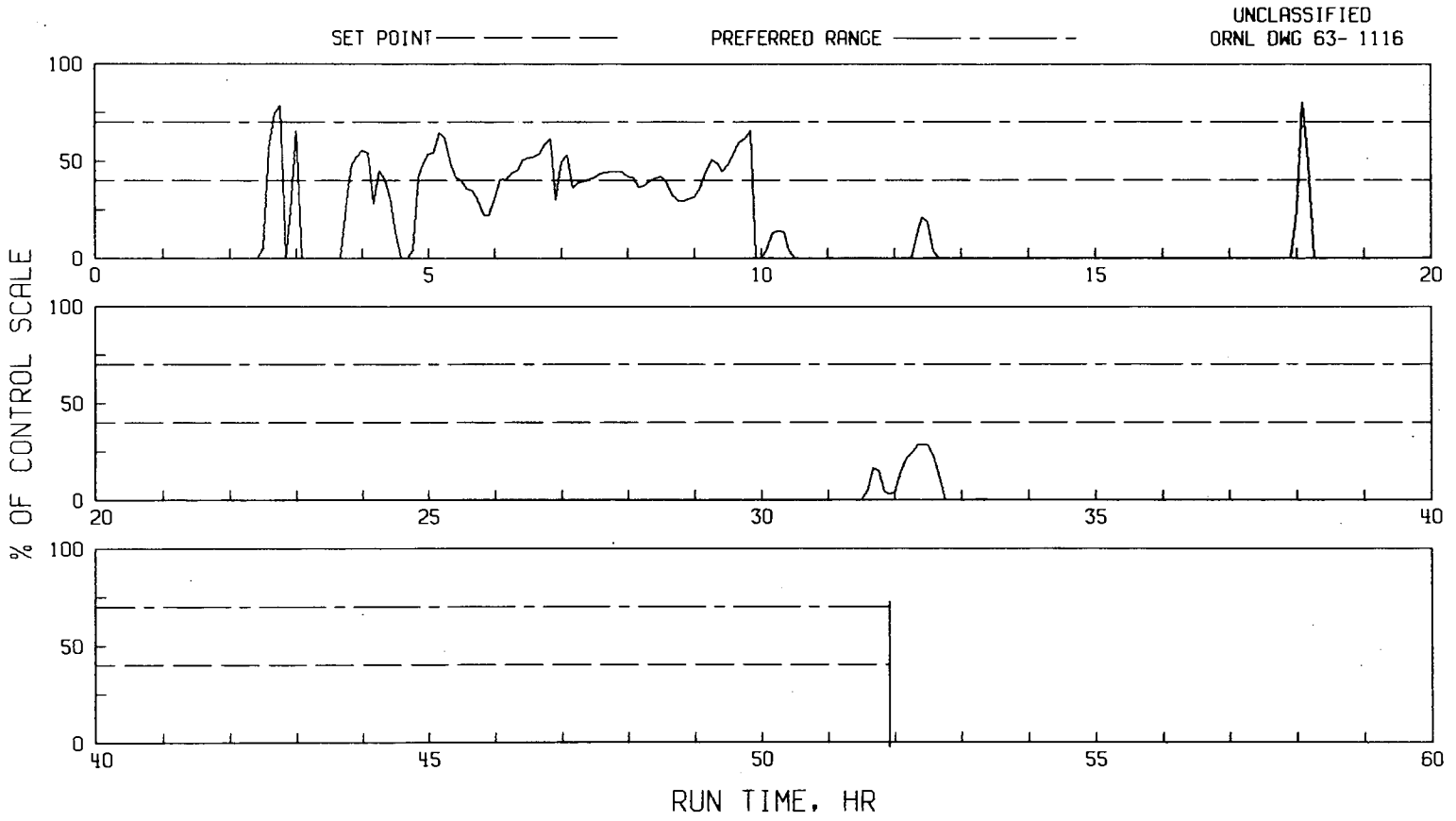

Fig. 4.9 Evaporator Vapor Conductivity Controller. Waste Calcination Test 78. Continuous Evaporation. Purex FTW-65.

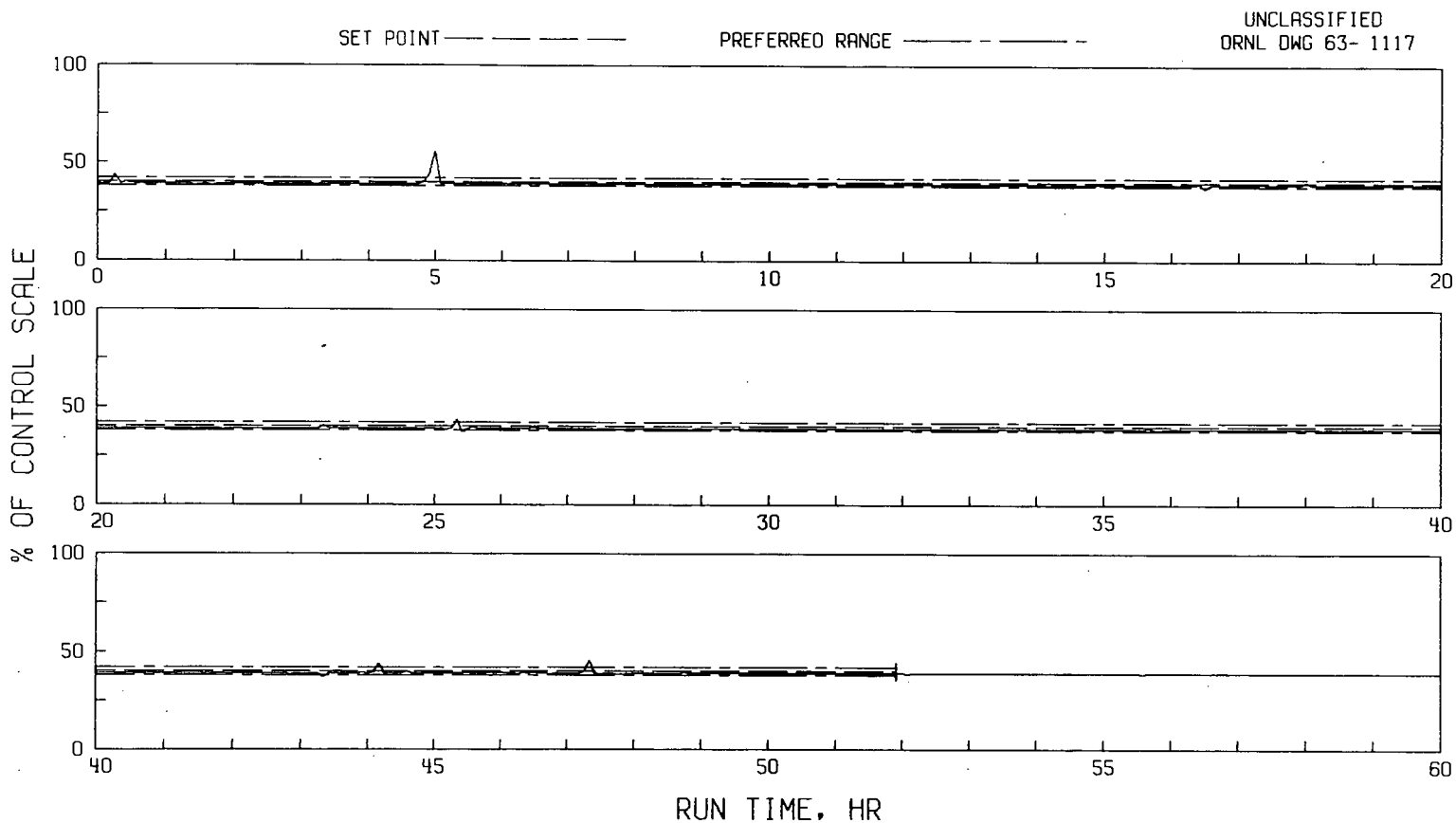

Fig. 4.10 Evaporator Vapor Pressure Controller. Waste Calcination Test 78. Continuous Evaporation. Purex FTW-65.

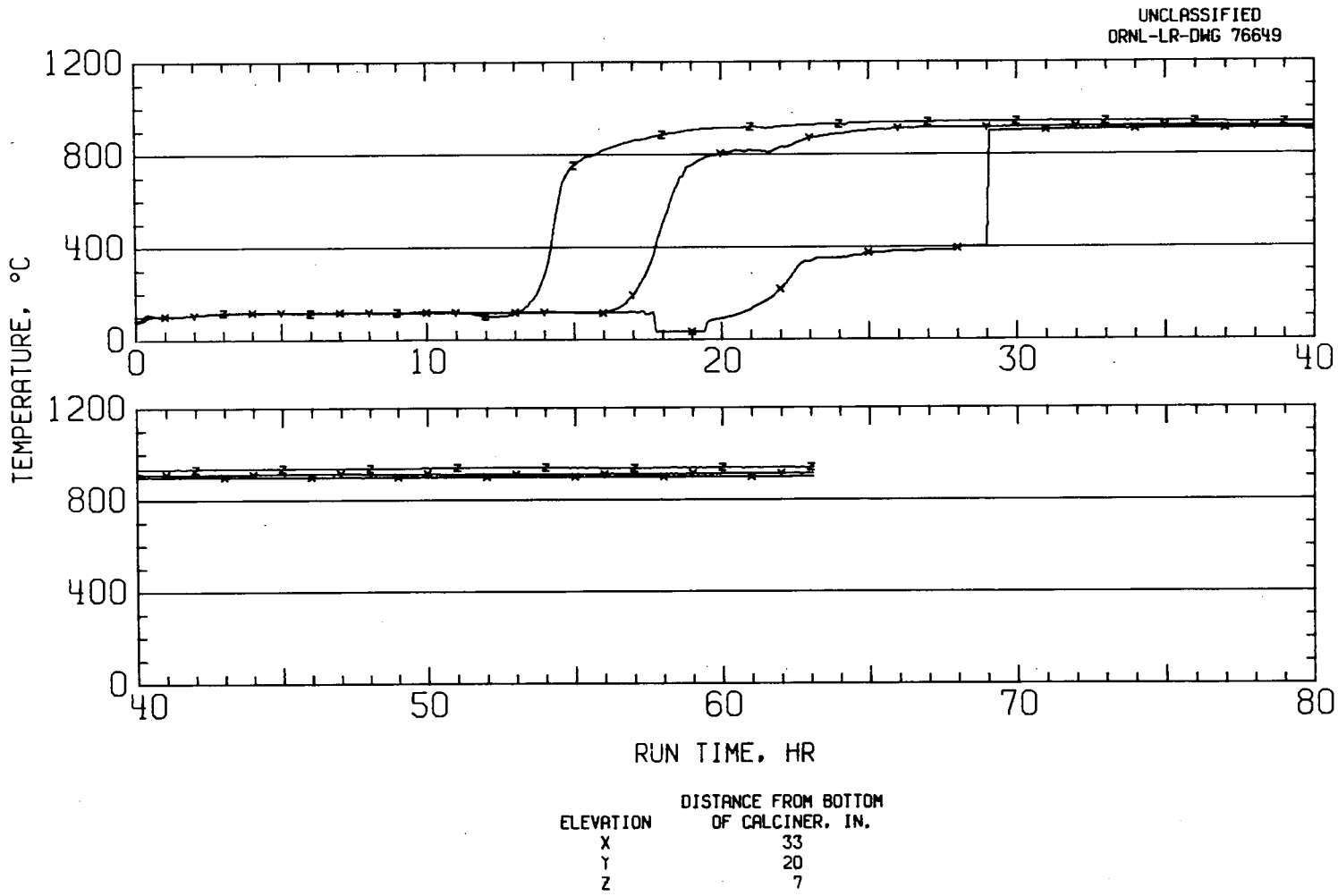

Fig. 4.11 Calciner Centerline Temperatures. Run No. 77.

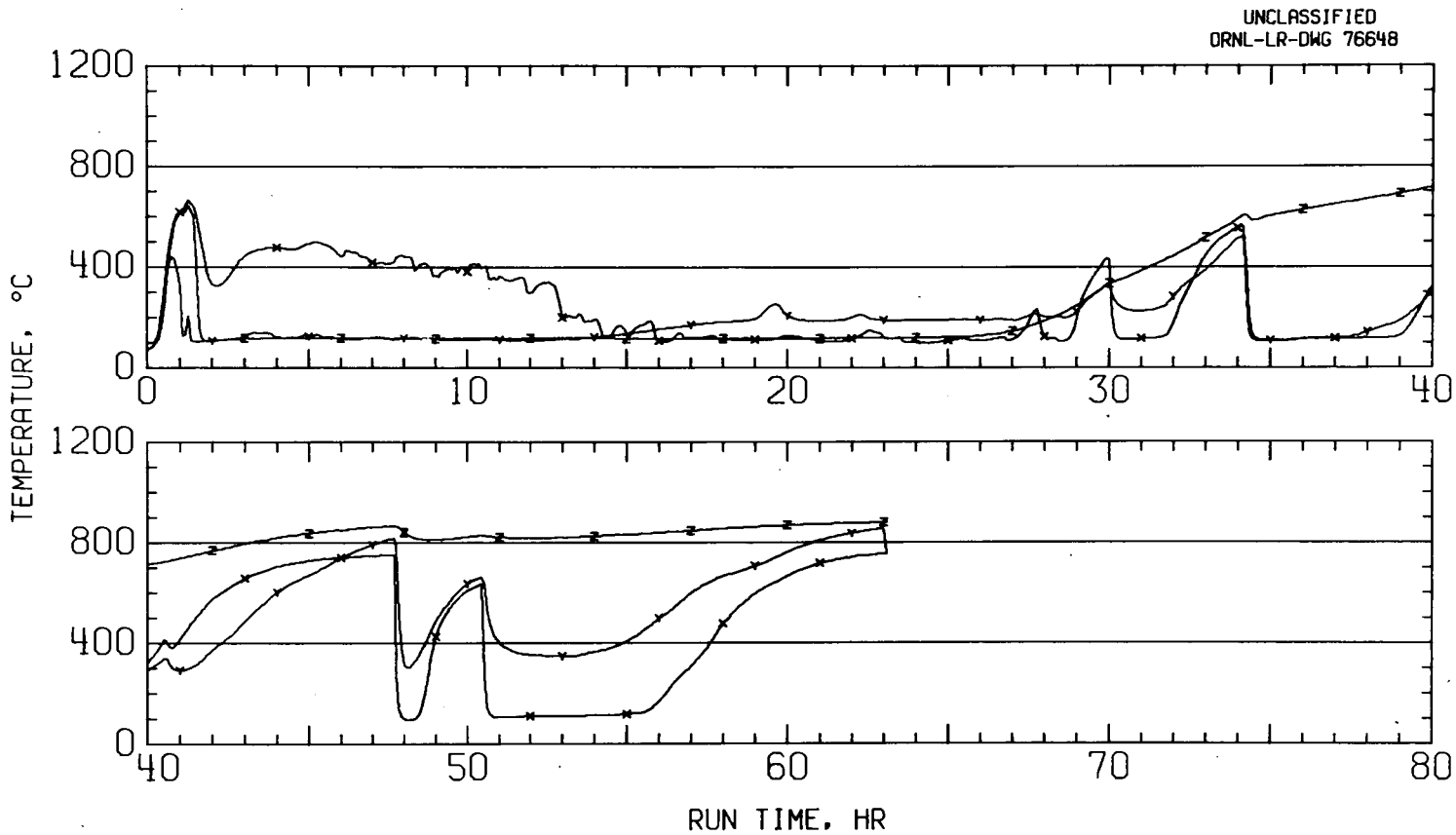

ELEVATION	DISTANCE FROM BOTTOM OF CALCINER, IN.
X	70
Y	58
Z	46

Fig. 4.12 Calciner Centerline Temperatures. Run No. 77.

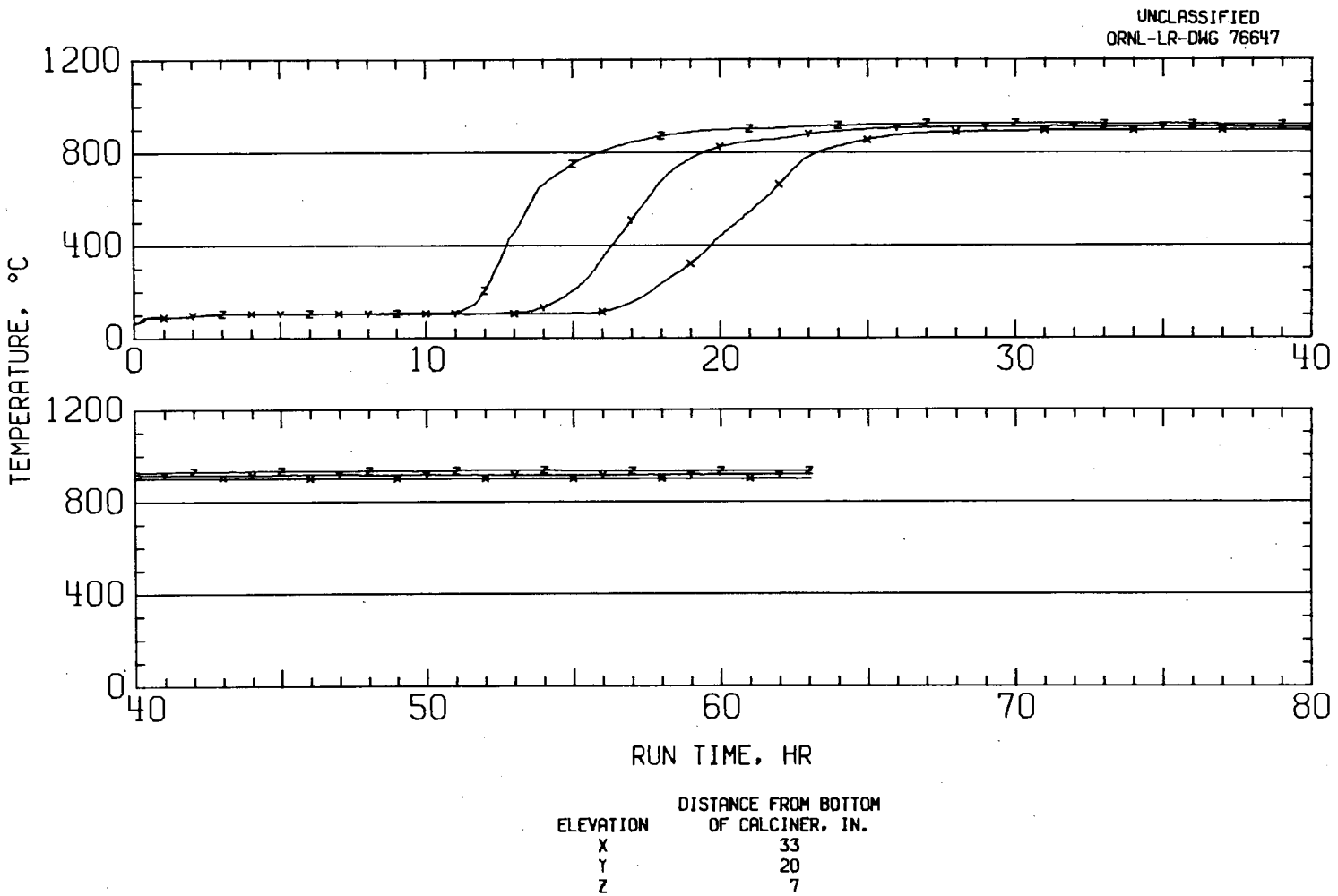

Fig. 4.13 Temperatures Inside Calciner Near Wall. Run No. 77.

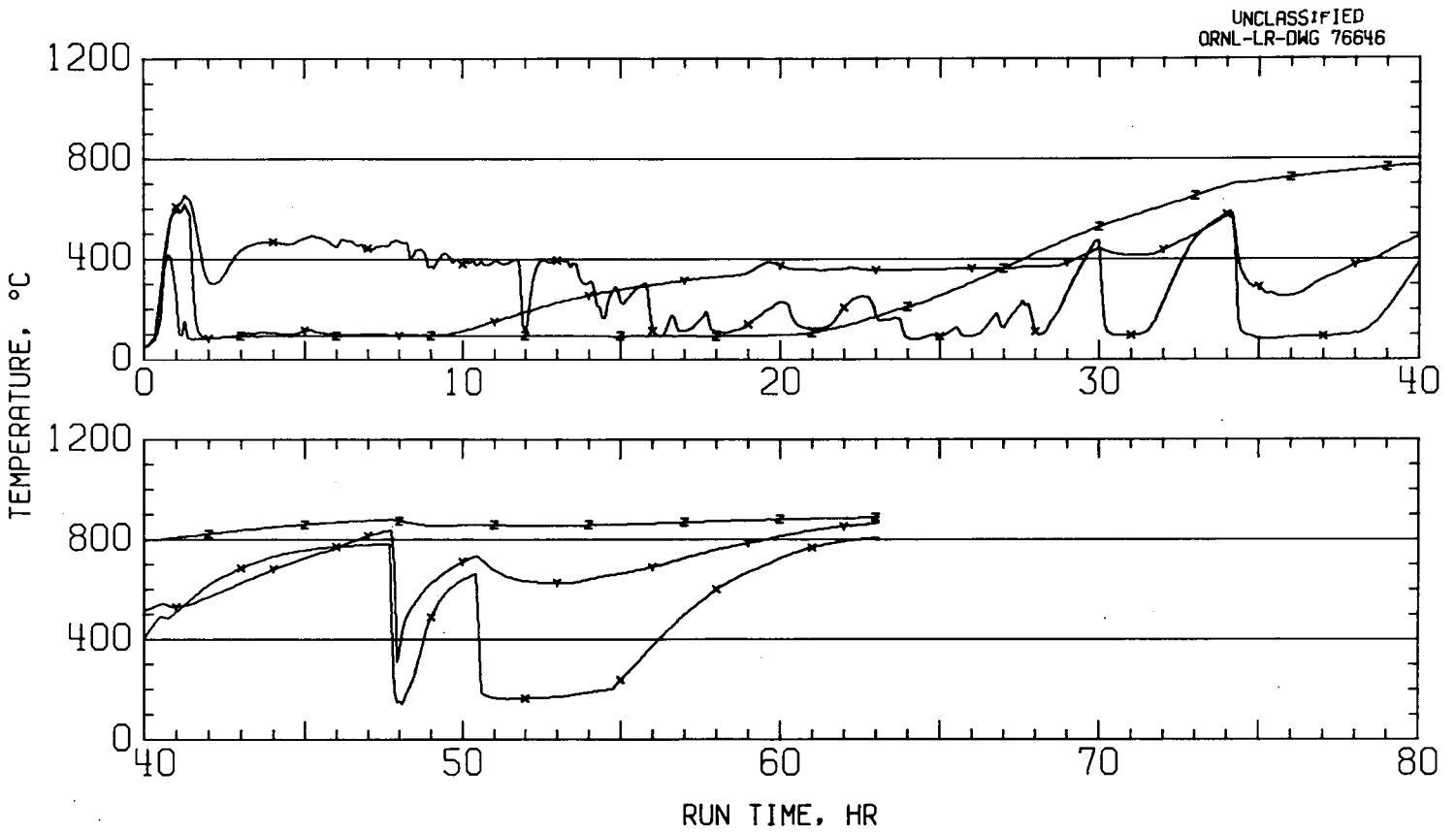

ELEVATION	DISTANCE FROM BOTTOM OF CALCINER, IN.
X	70
Y	58
Z	46

Fig. 4.14 Temperatures Inside Calciner Near Wall. Run No. 77.

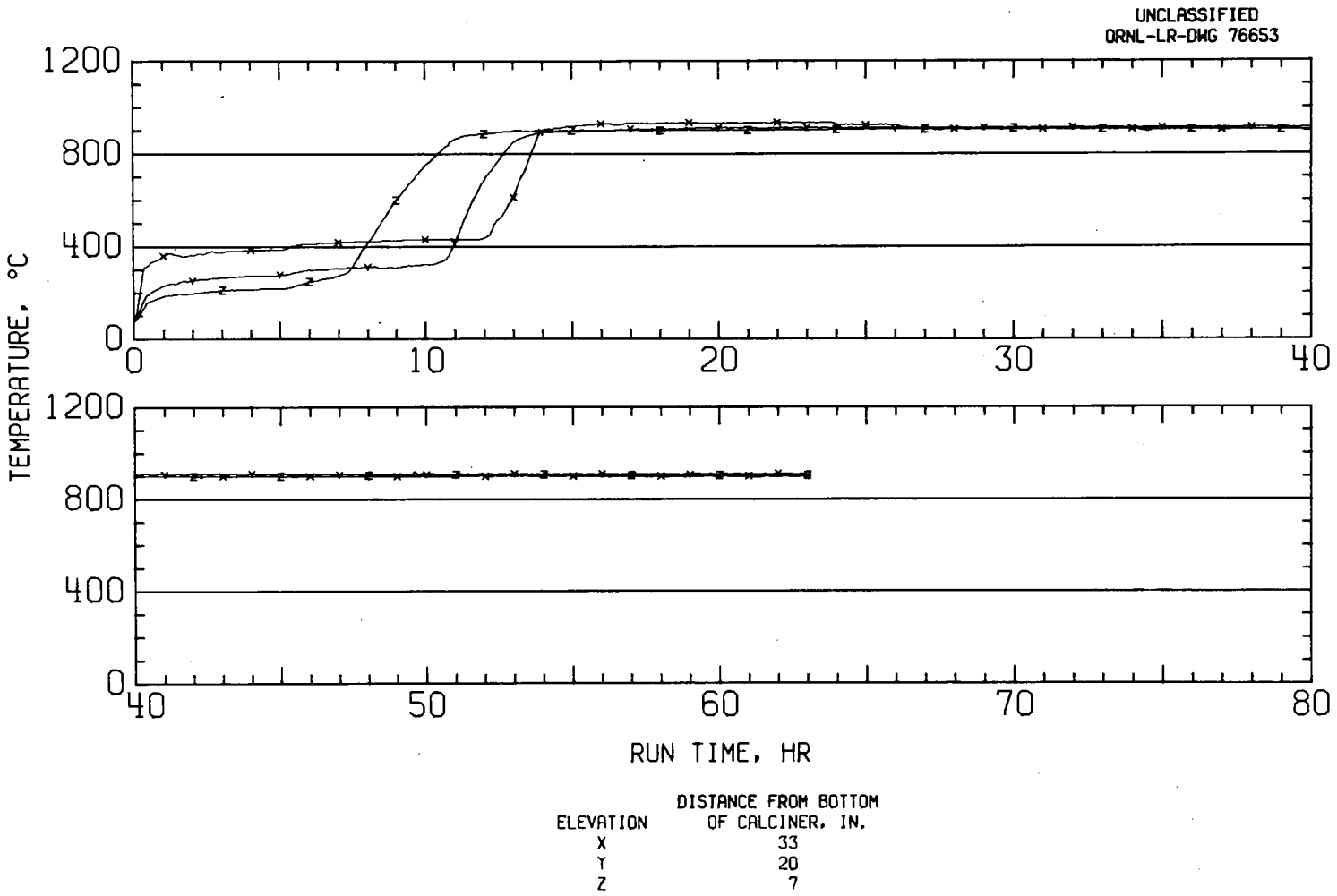

Fig. 4.15 Calciner Skin Temperatures. Run No. 77.

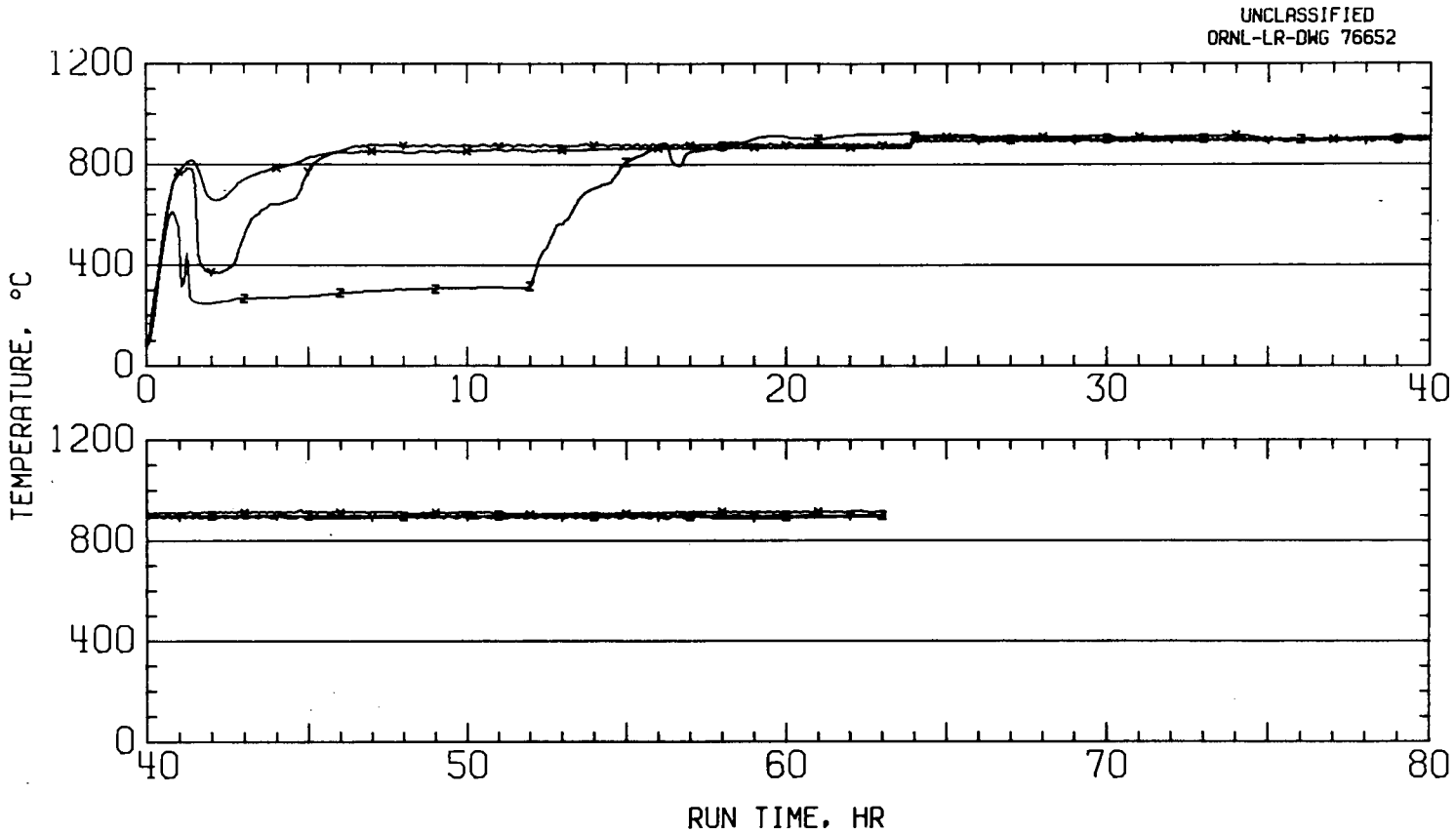

ELEVATION	DISTANCE FROM BOTTOM OF CALCINER, IN.
X	70
Y	58
Z	46

Fig. 4.16 Calciner Skin Temperatures. Run No. 77.

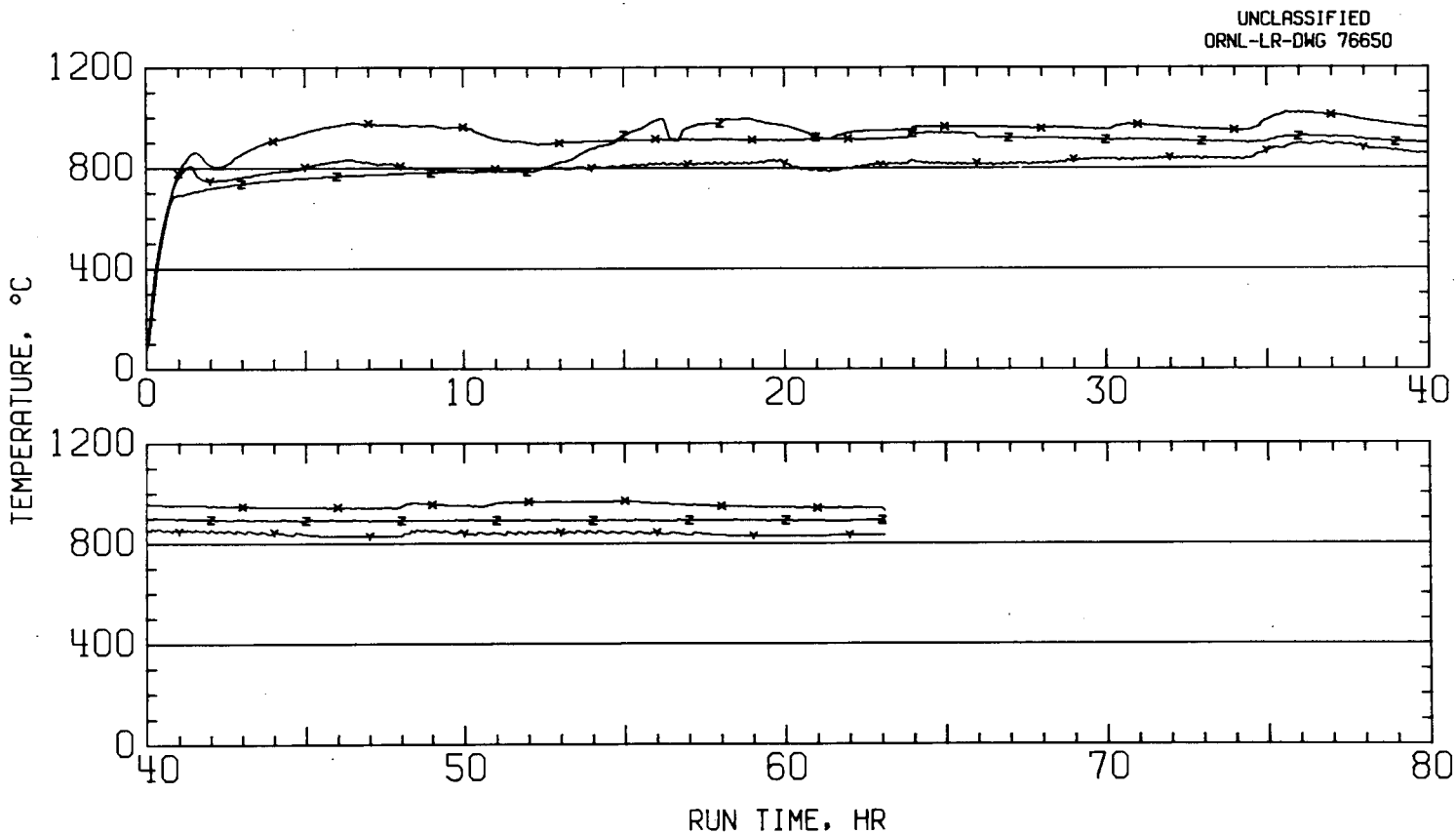

ELEVATION	DISTANCE FROM BOTTOM OF CALCINER, IN.
X	70
Y	58
Z	46

Fig. 4.17 Calciner Furnace Temperatures. Run No. 77.

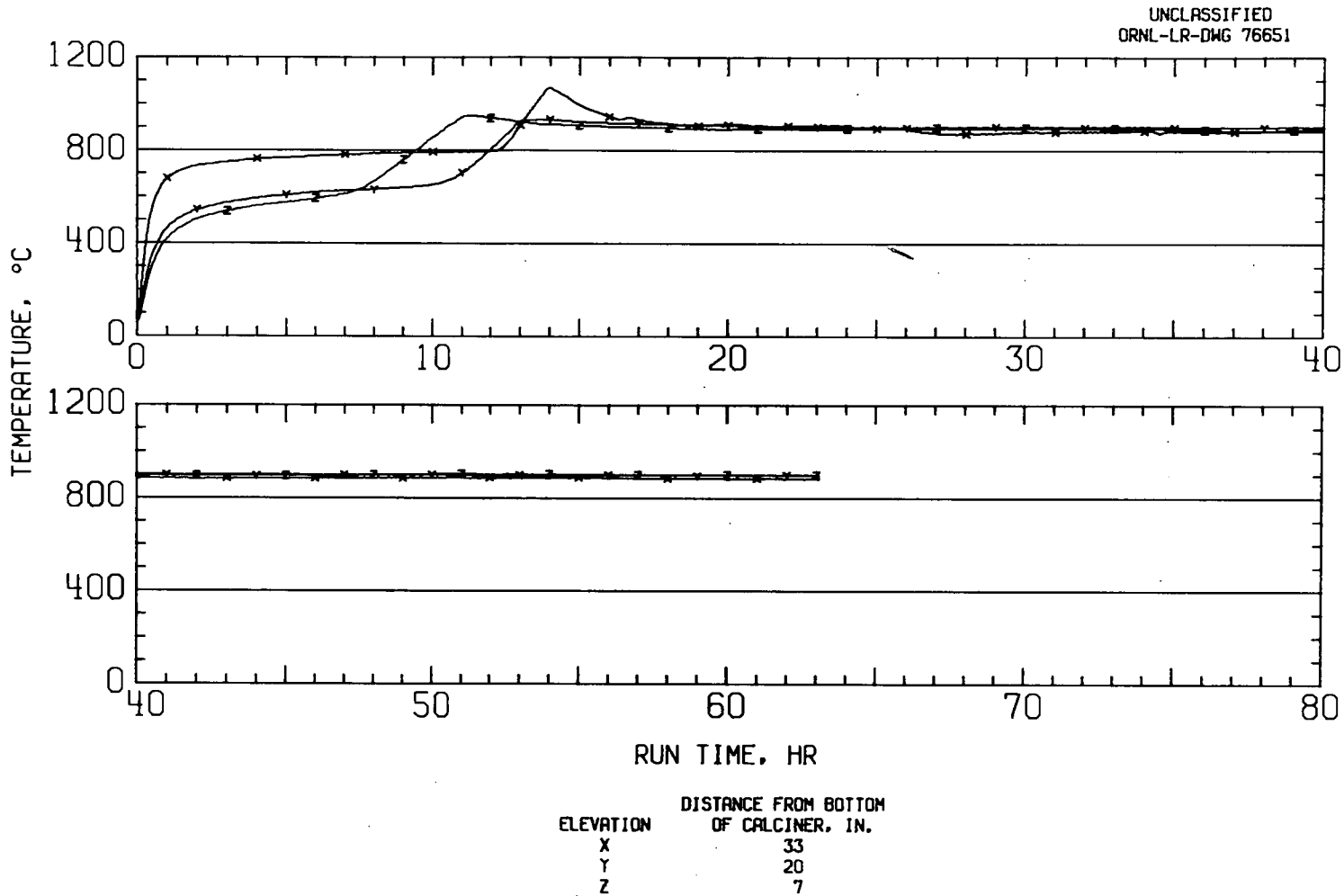

Fig. 4.18 Calciner Furnace Temperatures. Run No. 77.

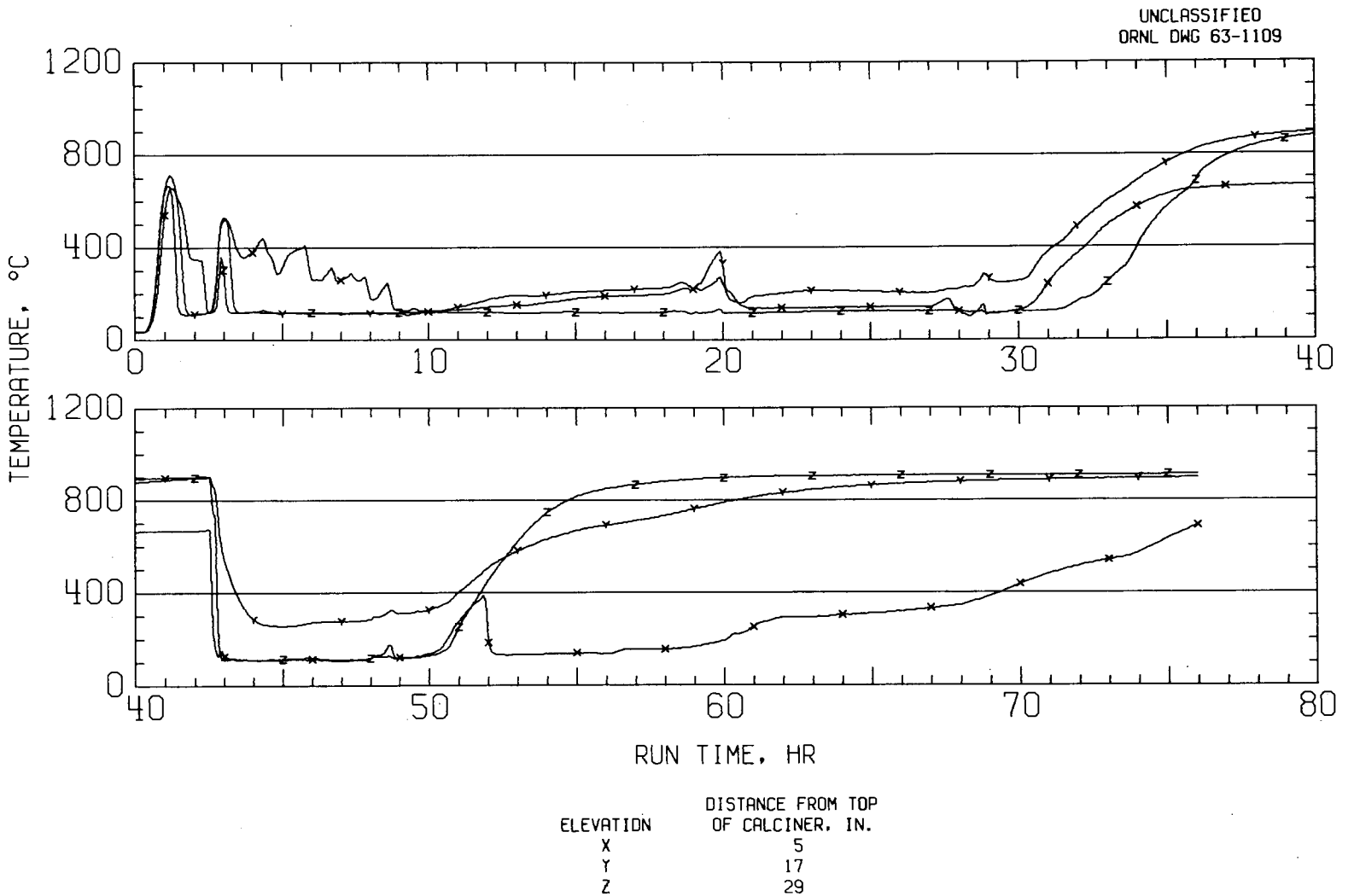

Fig. 4.19 Calciner Centerline Temperatures. Run No. 78.

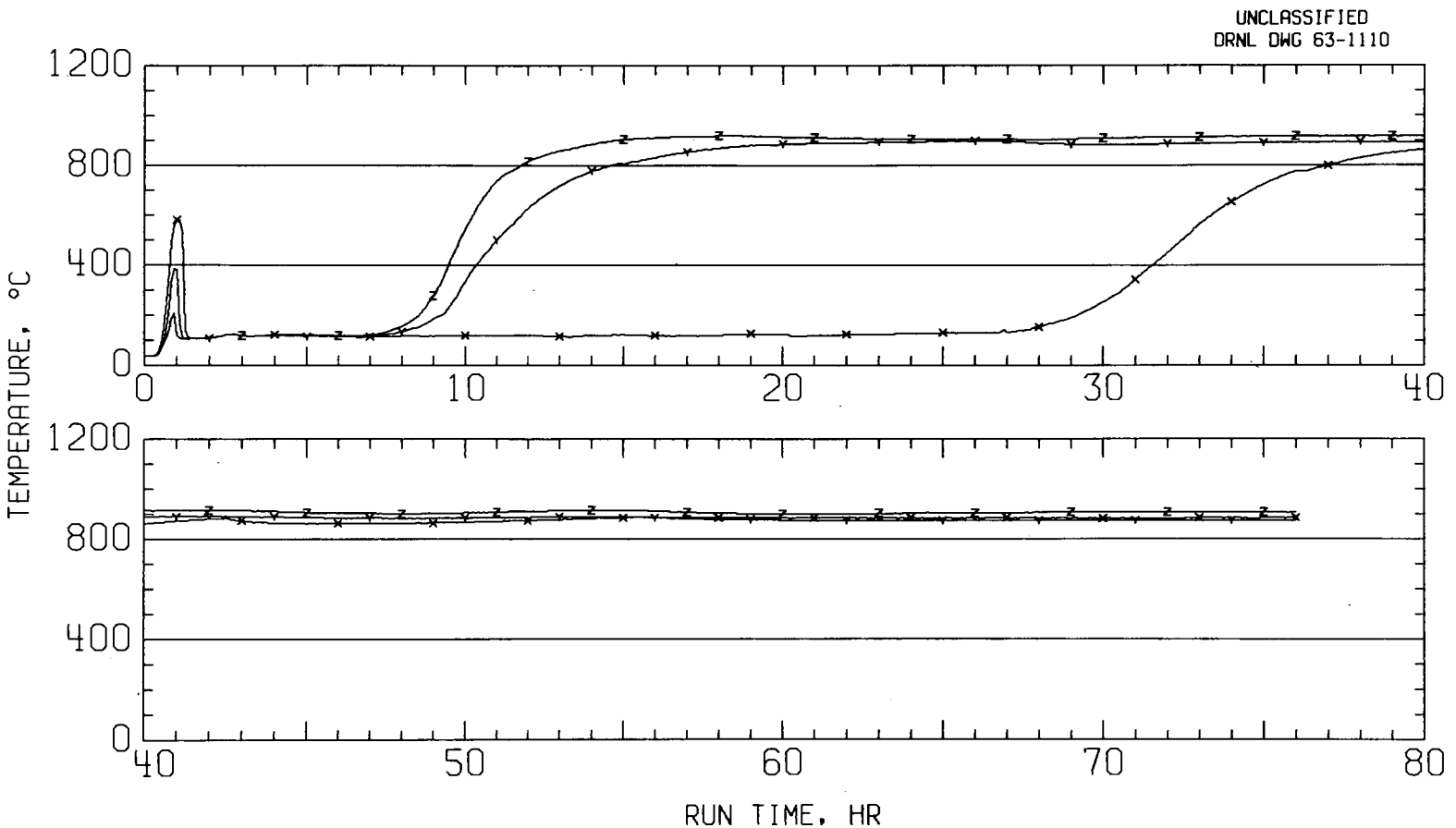

ELEVATION	DISTANCE FROM TOP OF CALCINER, IN.
X	42
Y	55
Z	68

Fig. 4.20 Calciner Centerline Temperatures. Run No. 78.

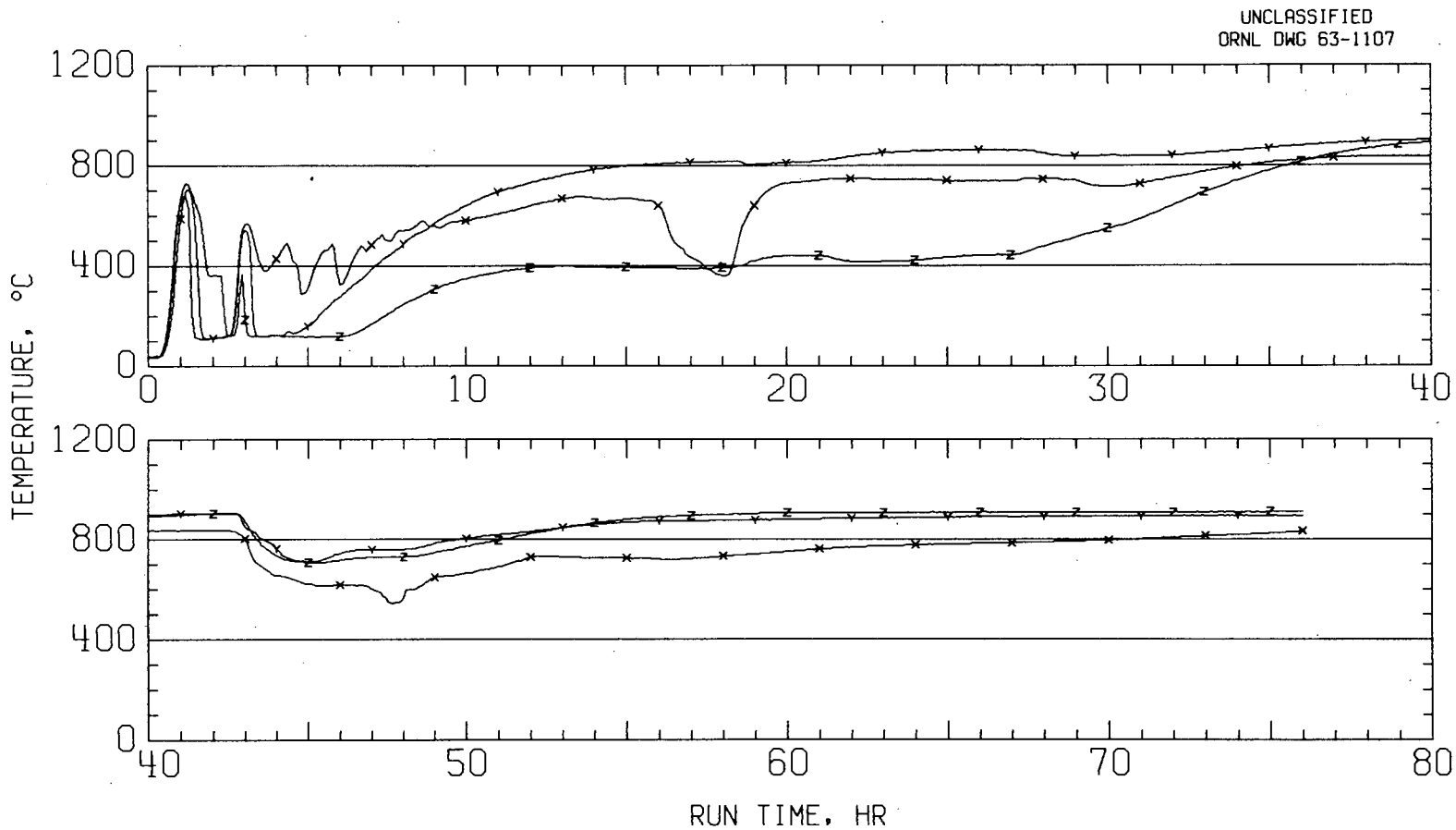

ELEVATION	DISTANCE FROM TOP OF CALCINER, IN.
X	5
Y	17
Z	29

Fig. 4.21 Temperatures Inside Calciner Near Wall. Run No. 78.

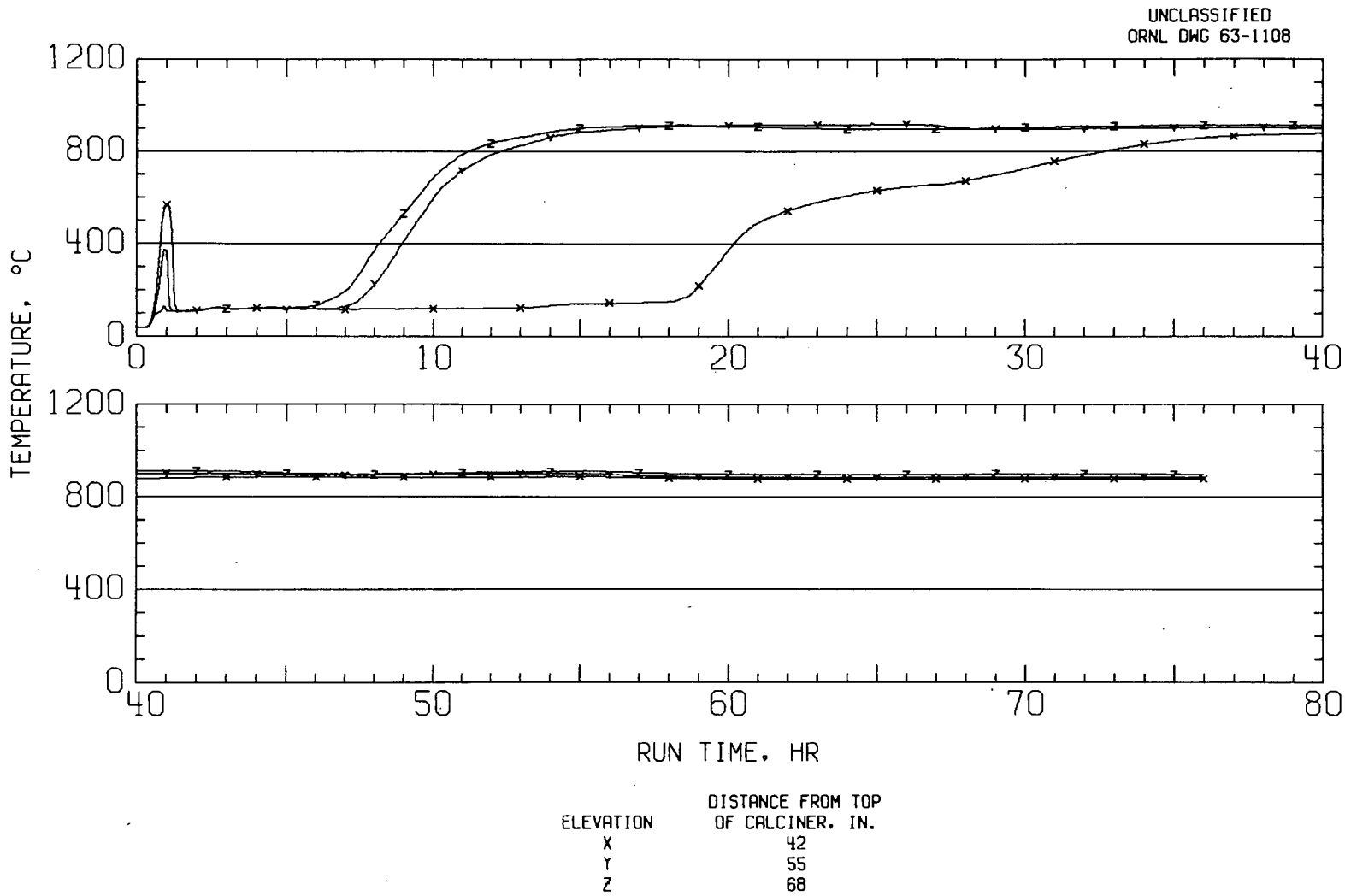

Fig. 4.22 Temperatures Inside Calciner Near Wall. Run No. 78.

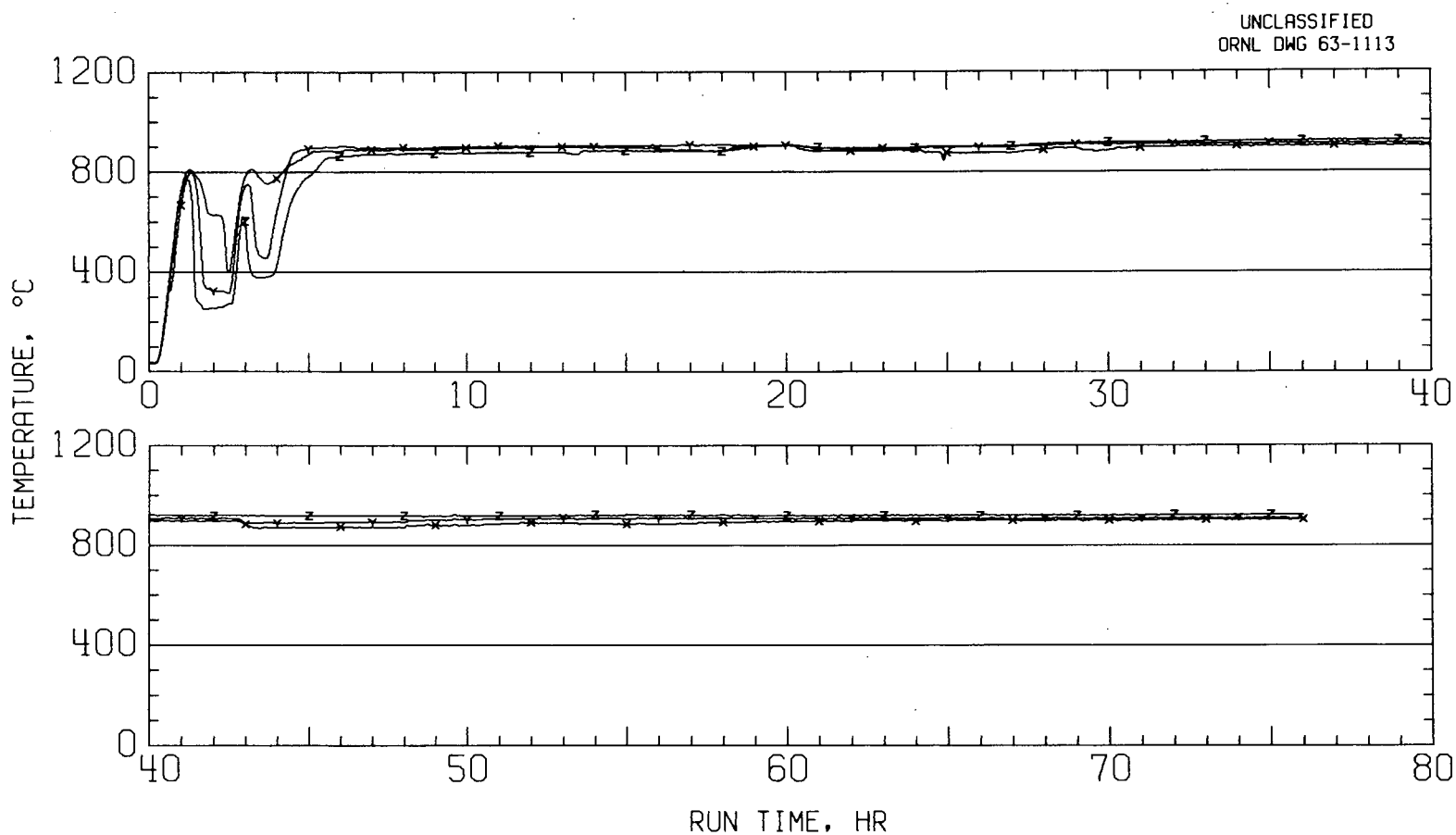

ELEVATION	DISTANCE FROM TOP OF CALCINER, IN.
X	5
Y	17
Z	29

Fig. 4.23 Calciner Skin Temperatures. Run No. 78.

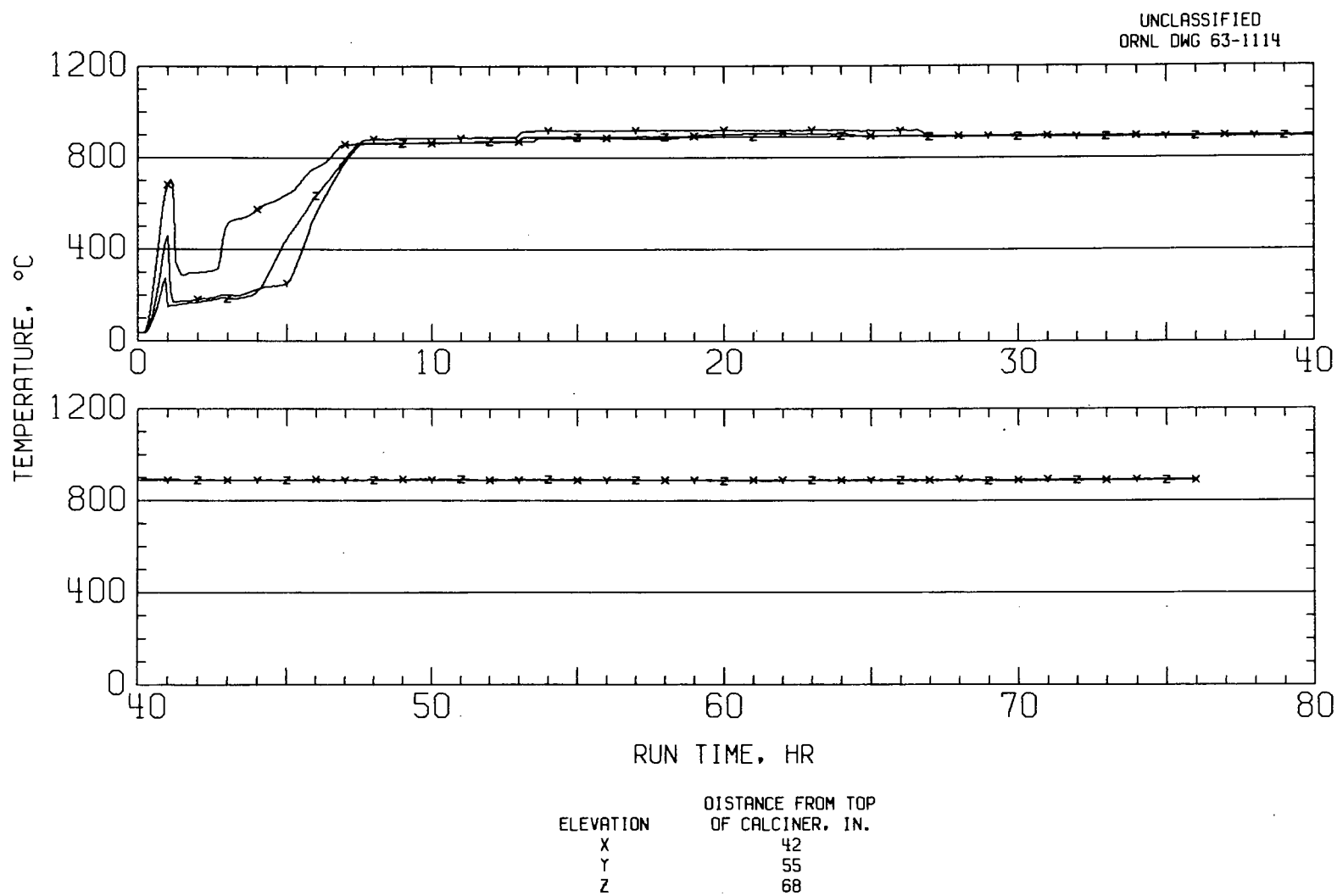

Fig. 4.24 Calciner Skin Temperatures. Run No. 78.

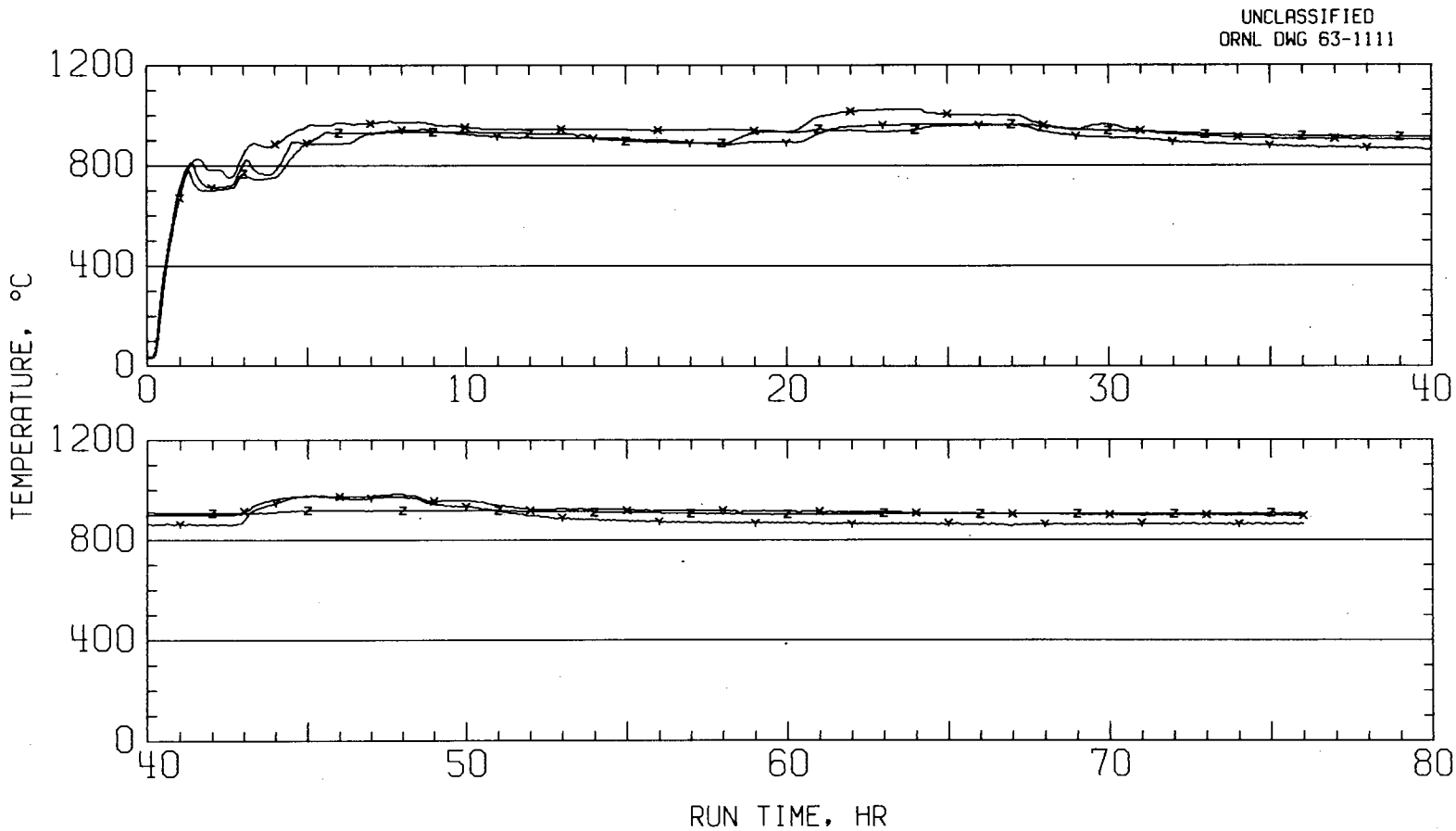

ELEVATION	DISTANCE FROM TOP OF CALCINER, IN.
X	5
Y	17
Z	29

Fig. 4.25 Calciner Furnace Temperatures. Run No. 78.

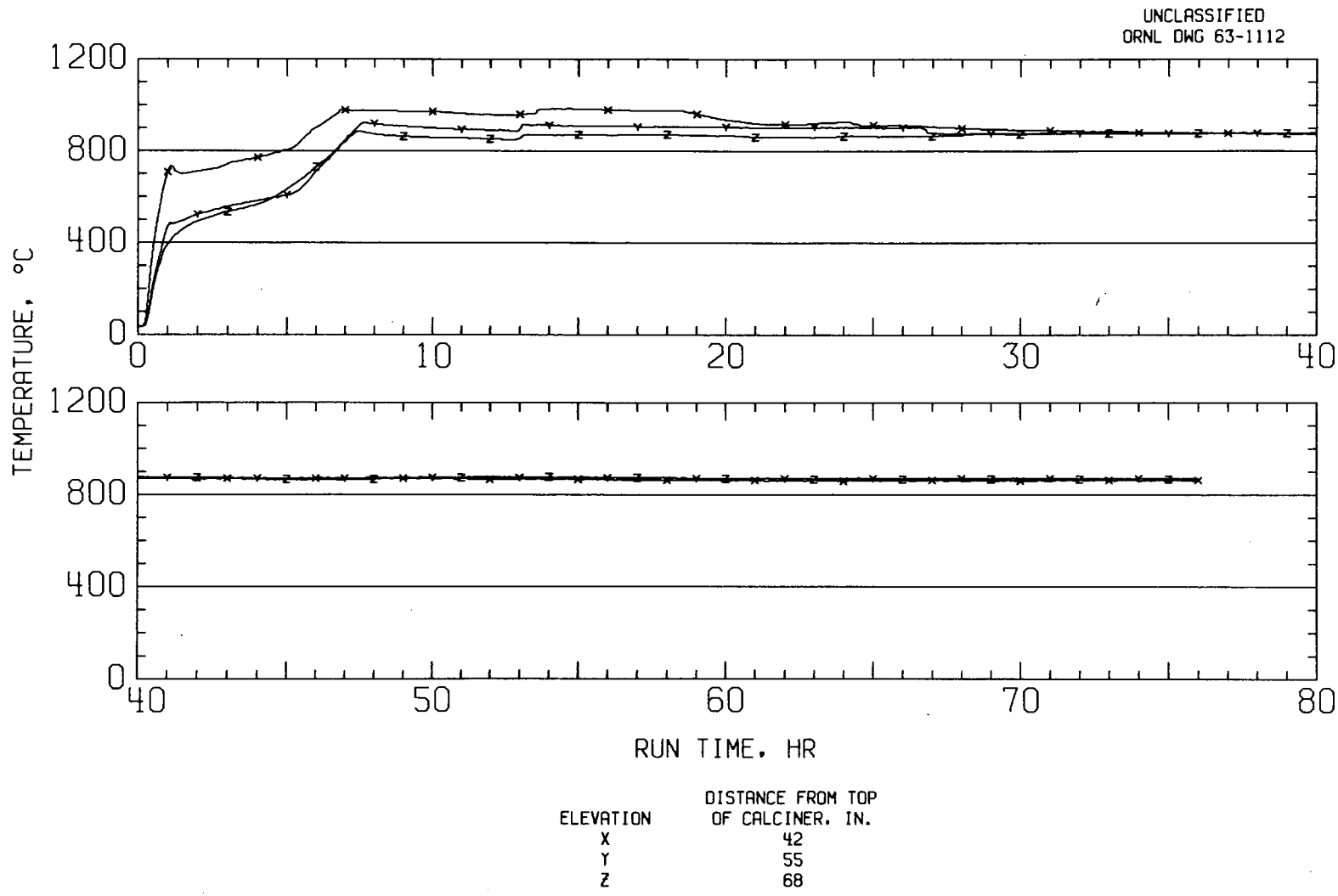

Fig. 4.26 Calciner Furnace Temperatures. Run No. 78.

DISTRIBUTION

1. L. G. Alexander (Y-12)
2. E. L. Anderson (AEC Washington)
3. A. L. Babb (U. of Washington)
4. F. P. Baranowski (AEC Washington)
5. W. G. Belter (AEC Washington)
6. S. Bernstein (Paducah)
7. R. E. Blanco
8. J. O. Blomeke
9. J. C. Bresee
10. R. E. Brooksbank
11. K. B. Brown
12. F. R. Bruce
13. J. A. Buckham (ICPP)
14. W. D. Burch
15. W. H. Carr
16. G. I. Cathers
17. J. M. Chandler
18. J. T. Christy (HOO)
19. W. E. Clark
20. C. R. Cooley (HAPO)
21. K. E. Cowser
22. F. L. Culler, Jr.
23. W. Davis, Jr.
24. O. C. Dean
25. D. E. Ferguson
26. L. M. Ferris
27. R. J. Flanary
28. E. R. Gilliland (MIT)
29. H. E. Goeller
30. M. J. Googin (Y-12)
31. H. B. Graham
32. A. T. Gresky
33. P. A. Haas
34. M. J. Harmon (HAPO)
35. F. E. Harrington
36. L. P. Hatch (BNL)
37. O. F. Hill (HAPO)
38. J. M. Holmes
39. R. W. Horton
40. E. R. Irish (HAPO)
41. G. Jasny (Y-12)
42. H. F. Johnson
43. W. H. Jordan
44. S. H. Jury
45. K. K. Kennedy (IDO)
46. B. B. Klima
47. E. Lamb
48. D. M. Lang
49. S. Lawroski (ANL)
50. R. E. Leuze
51. J. A. Lieberman (AEC Washington)
52. R. B. Lindauer
53. A. P. Litman
54. J. T. Long
55. B. Manowitz (BNL)
56. J. L. Matherne
57. J. A. McBride (ICPP)
58. J. P. McBride
59. W. T. McDuffee
60. R. A. McGuire (ICPP)
61. R. P. Milford
62. E. C. Moncrief
63. J. W. Morris (SRP)
64. J. W. Nehls (AEC ORO)
65. C. M. Nicholls (AERA, Harwell, Eng.)
66. E. L. Nicholson
67. F. L. Parker
68. J. R. Parrott
69. F. S. Patton, Jr. (Y-12)
70. H. Pearlman (AI)
71. A. M. Platt (HAPO)
72. R. H. Rainey
73. W. H. Rease (HAPO)
74. J. T. Roberts (IAEA, Vienna)
75. K. L. Rohde (ICPP)
76. C. A. Rohrmann (HAPO)
77. L. Rubin (RAI)
78. A. D. Ryon
79. W. F. Schaffer, Jr.
80-82. E. M. Shank
83. M. J. Skinner
84. C. M. Slansky (ICPP)
85. S. H. Smiley (ORGDP)
86. M. Smutz (Ames Lab, Ames, Ia.)
87. J. I. Stevens (ICPP)
88. C. E. Stevenson (ANL, Idaho Falls)
89. K. G. Steyer (General Atomics)
90. J. C. Suddath
91. J. A. Swartout
92. C. D. Tabor (Goodyear Atomic)
93. F. M. Tench (Y-12)
94. V. R. Thayer (duPont, Wilmington)
95. W. E. Unger
96. F. M. Warzel (ICPP)
97. C. D. Watson
98-127. M. E. Whatley
128. G. C. Williams
129. R. H. Winget
130. R. G. Wymer
131-132. Central Research Library
133-136. Laboratory Records
137. Laboratory Records (RC)
138-139. Document Reference Section
140. Research and Development Div. (ORO)
141. ORNL Patent Office
142-156. DTIE